CHAPTER ONE

# A Sturmian Approach to Photoionization of Molecules

**Carlos Mario Granados-Castro**[*,†,1], **Lorenzo Ugo Ancarani**[*,1], **Gustavo Gasaneo**[†,‡], **Dario M. Mitnik**[‡,§]

[*]Equipe TMS, UMR CNRS 7565, ICPM, Université de Lorraine, 57078 Metz, France
[†]Departamento de Física, Universidad Nacional del Sur, 8000 Bahía Blanca, Buenos Aires, Argentina
[‡]Consejo Nacional de Investigaciones Científicas y Técnicas CONICET, Argentina
[§]Instituto de Astronomía y Física del Espacio (IAFE) and Departamento de Física, Universidad de Buenos Aires, C1428EGA Buenos Aires, Argentina
[1]Corresponding authors: e-mail address: carlos.mario-granados.castro@univ-lorraine.fr; ugo.ancarani@univ-lorraine.fr

## Contents

1. Introduction 4
2. Generalities 6
3. Examples Taken from the Literature 8
   3.1 $H_2$ 9
   3.2 $N_2$ 10
   3.3 $CO_2$ 11
   3.4 $C_6H_6$ 12
4. Survey of Theoretical Methods 13
   4.1 CI 13
   4.2 Hartree–Fock Methods 13
   4.3 Density Functional Theory 14
   4.4 Complex Methods 15
   4.5 Linear Algebraic Method 16
   4.6 Multi-Scattering 17
   4.7 Plane-Wave-Based Methods 18
   4.8 *R*-Matrix Method 19
   4.9 Random Phase Approximation 20
   4.10 Stieltjes–Tchebycheff Technique 21
   4.11 The Kohn Variational Method 21
   4.12 The Schwinger Variational Method 23
   4.13 Crank–Nicolson 25
5. Sturmian Approach 25
   5.1 Generalized Sturmian Functions 25
   5.2 Sturmian Approach to Photoionization Process 27
   5.3 Results for Molecules 34
6. Conclusions 39

*Advances in Quantum Chemistry*, Volume 73
ISSN 0065-3276
http://dx.doi.org/10.1016/bs.aiq.2015.06.002

Acknowledgments 41
Appendix. List of Photoionization Calculations for Different Molecules 42
References 44

## Abstract

An accurate theoretical description of photoionization processes is necessary in order to understand a wide variety of physical and chemical phenomena and allows one to test correlation effects of the target. Compared to the case of many-electron atoms several extra challenges occur for molecules. The scattering problem is generally multicenter and highly noncentral. The molecular orientation with respect to the polarization of the radiation field must also be taken into account. These features make the computational task much more cumbersome and expensive than for atomic targets. In order to calculate cross sections, one needs to describe the ejected electron with a continuum wavefunction with appropriate Coulomb asymptotic conditions. Making a number of initial approximations, many different theoretical/numerical methods have been proposed over the years. However, depending on the complexity of the molecule, agreement among them is not uniform and many features of the experimental data are not so well reproduced. This is illustrated through a number of examples. In order to have a global theoretical overview, we present a survey of most of the methods available in the literature, indicating their application to different molecules. Within a Born–Oppenheimer, one-center expansion and single active electron approximation, we then introduce a Sturmian approach to describe photoionization of molecular targets. The method is based on the use of generalized Sturmian functions for which correct boundary conditions can be chosen. This property makes the method computationally efficient, as illustrated with results for $H_2O$, $NH_3$, and $CH_4$.

## 1. INTRODUCTION

The quantum description of both bound and unbound orbitals is necessary to study collisions with atoms and molecules. The study of single photoionization (PI) provides an indirect tool to test our capacity to describe the target before and after the interaction correctly and thus correlation and many-body effects. PI plays an important role beyond atomic and molecular physics, since it has a wide variety of applications, such as astrophysics, [1–3] planetary,[4–6] atmospheric,[7–8] plasma,[9–11] or medical physics.[12,13] Also PI helps to understand different processes in surfaces, such as structural changes upon surface adsorption, quantifying the relationship between shape resonances and the bond lengths[14–17]; or to characterize the relation between gas, chemisorbed and solid-state phases in surface reactions.[18–21]

In the last few years, a Sturmian approach[22–23] has been introduced to study single and double ionization of atoms induced by electron[24] or

photon[25] impact. It is the purpose of this contribution to extend, implement and apply such an approach to the single PI of molecular targets. The Hamiltonian for molecules being generally multicenter and highly noncentral makes the problem more difficult than for atomic targets. Indeed, the absence of any spherical symmetry couples different angular momenta from different atomic orbitals (AOs) that form the molecular orbitals (MOs) and thus convergence of "traditional" methods is considerably more difficult to achieve. Additionally, there are various many-body effects that can be important in ionization processes, such as the relaxation of all MOs, due to the creation of a hole (ionized electron), or the change of the remaining pair correlation energies because of such relaxation. An issue which does not arise in PI of atoms is the orientation of the molecular target. In most experiments, the molecule is randomly oriented and this must be taken into account within the theoretical calculations.

When leaving an atomic or molecular target, an ionized electron needs to be described accurately by a continuum wavefunction, which has well defined boundary conditions. Over the years, quite a few methods have been proposed and applied successfully to atoms. The extension of these methods and their computational codes to molecular targets is not straightforward, as several complications arise beyond the many-body nature of the problem and not all of them can provide the correct asymptotic form. Different approaches have been applied to a large variety of molecules ranging from the smallest one, $H_2$, up to, e.g., DNA bases. The success of each method depends on the studied molecule and photon energy range, the validity of some approximations and possibly on convergence issues or limitations related to the numerical implementation.

Except for small molecules, experimental data are not so abundant and do not always span the whole photoelectron energy range; they therefore do not permit a full assess to the quality of different theoretical descriptions. As several theories often disagree with each other and with experimental data, especially close to threshold, we made a survey of most existing methods applied to PI in molecules. For each, we briefly indicate the main ingredients, the advantages and possible limitations. We also found useful to draw a list (rather complete to the best of our knowledge) of all molecules for which PI has been investigated theoretically.

In order to calculate the transition amplitudes for single PI in atomic or molecular systems, many considerations must be taken into account. Usually the starting point is the treatment of the ionized electron as a one-electron function, the one-center expansion (OCE). In many cases, the vibrational

structure of the molecule can be ignored, especially in high-energy collisions, justifying the use of the Born–Oppenheimer (BO) approximation. Also, in order to simplify the calculations, the frozen core (FC) approximation and the static exchange approximation (SEA) are considered. It is within this frame, together with a model molecular potential, that we implement the generalized Sturmian approach. In the literature, several Sturmian function implementations exist, as reviewed, e.g., in the introductions of Refs. 22 and 23. Similarly to previous publications on scattering studies (see the recent review 22 and references therein), in this contribution we shall name *Generalized Sturmian Functions* (GSF) those defined in Section 5.1; note that other authors use the same terminology to define a different class of Sturmian functions. One of the advantages of such a method is that it ensures that the continuum wavefunction has the correct asymptotic behavior.[22] To assess the validity of our approach, we will compare the calculated PI cross sections for a number of small molecules with theoretical and experimental data found in the literature.

The rest of this paper is organized as follows. We start with some generalities on PI in Section 2; we continue in Section 3 with a brief panorama of what sort of agreement one observes in the literature between theoretical and experimental cross sections. In Section 4, we present a survey of existing theoretical methods used to investigate molecular PI. In Section 5, we introduce the Sturmian approach, and compare our results for PI of $H_2O$, $NH_3$, and $CH_4$ to several theoretical and experimental data.

Atomic units ($\hbar = e = m_e = 1$) are assumed throughout, unless stated otherwise.

## 2. GENERALITIES

In the study of the interaction of a radiation field (a photon) with a molecular target several processes may occur. Consider a photon of energy $E_\gamma = \hbar\omega$, such that $E_\gamma > I_0$, where $I_0$ is the ionization potential of the molecule. Once it strikes a polyatomic molecule RA in an initial vibrational state $\nu_0$ (R is the polyatomic radical and A is an individual atom), the different outcomes may be

$$\hbar\omega + \mathrm{RA}(\nu_0) \rightarrow \begin{cases} \mathrm{RA}^+ + \mathrm{e}^-(\ell) & \text{Photoionization,} \\ \mathrm{R}^* + \mathrm{A}^* & \text{Photodissociation,} \\ \mathrm{R}^* + \mathrm{A}^{+*} + \mathrm{e}^-(\ell) & \text{Dissociative photoionization.} \end{cases} \quad (1)$$

If we have a dissociation process, the final products can be in an excited state. If we have an ejected electron, called photoelectron, it has a defined angular momentum $\ell$. In this contribution, we will concentrate only on single PI which can be considered as a "half-scattering" processes. It involves a bound-free transition for which one needs to know only the initial state $\mathbf{\Psi}_0$ (energy $E_0$) of the molecule, usually its ground state, and the final state of the ionized electron. The transition operator, that connects both initial and final states, is described semi-classically via the dipolar approximation; the dipolar operator in both length (L) and velocity (V) gauges reads

$$\widehat{D}^{(\mathrm{L})} = -\hat{\varepsilon} \cdot \mathbf{r}, \tag{2a}$$

$$\widehat{D}^{(\mathrm{V})} = -\hat{\varepsilon} \cdot \mathbf{p}, \tag{2b}$$

where $\hat{\varepsilon}$ gives the polarization of the field. In this work, we consider linear polarization along the $z$ direction.

The major task is to calculate accurately the wavefunction $\mathbf{\Psi}$ of the photoelectron, that is an electron in a continuum state of the ionized molecular target, with an energy $E = k^2/2$ defined by the energy of the incident photon $E = E_\gamma - I_0$. Such continuum wavefunctions are more difficult to calculate than the low-lying bound-states as they oscillate up to infinity. They are solutions of the time-dependent Schrödinger equation (TDSE) or the time-independent Schrödinger equation (TISE), with well defined properties. They must be regular at the origin of the coordinate system, and the asymptotic boundary conditions are given by the superposition of an incoming-wave Coulomb function plus an incoming spherical wave, generated by the non-Coulomb part of the molecular potential[26]

$$\lim_{r\to\infty} \mathbf{\Psi}^{(-)} \propto \mathrm{e}^{-i\left(kz + \frac{Z}{k}\ln k(r-z)\right)} + f\left(\hat{k},\hat{r}\right)\frac{1}{r}\mathrm{e}^{-i\left(kr - \frac{Z}{k}\ln(2kr)\right)}, \tag{3}$$

where $f\left(\hat{k},\hat{r}\right)$ is the transition amplitude and $Z = -1$ for an initial neutral target.

One quantity that is measurable experimentally is the PI cross section, defined theoretically as

$$\frac{\mathrm{d}\sigma}{\mathrm{d}E} = \frac{\pi \mathrm{e}^2}{m^2\hbar^2 c}\omega^{(\mathrm{g})}\left|\left\langle \mathbf{\Psi}_0 \middle| \widehat{D}^{(\mathrm{g})} \middle| \mathbf{\Psi} \right\rangle\right|^2, \tag{4}$$

where $\omega^{(\mathrm{L})} = E - E_0$ or $\omega^{(\mathrm{V})} = (E - E_0)^{-1}$ and $c$ is the speed of light.

In most experiments, it is difficult to determine the spatial orientation of the molecule in a given laboratory frame. Only a few advanced experimental techniques can perform a full angle-resolved spectroscopy, such as the one based on ultrashort pump-probe laser pulses[27,28] and the full kinematic experiments as COLTRIMS (cold target recoil ion momentum spectroscopy).[29] In most cases, therefore, one must consider a random orientation of the molecule when it interacts with the radiation field. To do that, two different coordinates systems, whose origin coincide with the center of mass of the target, are considered[30]: the laboratory frame, $\mathbf{r}'$, defined by the polarization axis of the electric field, and a molecular-fixed frame, $\mathbf{r}$, defined by the axis of highest symmetry. Let $\beta$ and $\alpha$ be the polar angles of this molecular axis with respect to the laboratory frame, and let the set of Euler angles $\hat{\mathfrak{R}} = (\alpha, \beta, \gamma)$ denote hereafter the molecular orientation. A rotation $\hat{\mathfrak{R}}$ will bring the molecular fixed frame into coincidence with the laboratory frame. The dipolar operator in length gauge (2a), for a linearly polarized field (axis $z$), in the laboratory frame is then

$$z' = \left(\frac{4\pi}{3}\right)^{1/2} r \sum_{\mu} Y_1^{\mu}(\hat{r}) \mathcal{D}^1_{0\mu}\left(\hat{\mathfrak{R}}\right), \tag{5}$$

where $\mathcal{D}^1_{0\mu}\left(\hat{\mathfrak{R}}\right)$ is the rotation matrix[31] that rotates the dipolar operator to the molecular frame. The rotated dipolar operator in velocity gauge follows a similar expression. In order to calculate a cross section for a randomly oriented molecule, we must calculate first the orientation-dependent transition amplitudes in Eq. (4) (see also Section 5.2) and then perform an angular average over $\hat{\mathfrak{R}}$, defined as

$$\int \mathrm{d}\hat{\mathfrak{R}} \equiv \frac{1}{8\pi^2} \int_0^{2\pi} \mathrm{d}\alpha \int_0^{\pi} \sin\beta \, \mathrm{d}\beta \int_0^{2\pi} \mathrm{d}\gamma \,, \tag{6}$$

of the square modulus of such transition amplitudes.

## 3. EXAMPLES TAKEN FROM THE LITERATURE

As mentioned in Section 1, many different theoretical methods and computational codes have been developed over the years to study PI in multielectron atoms. For molecules, many complications arise. The problem is highly noncentral and generally multicenter so that continuum wavefunctions are quite difficult to calculate. Additionally the vibrational

structure can have an important influence on the electronic structure and therefore on the PI itself.

To overcome all these complexities, additional to the "traditional" (FC) or the SEA, one starts to separate the electronic motion from that of the nuclei and this is done using the BO approximation. One may also implement the fixed nuclei (FN) approximation, and it is possible to go further and use the OCE, where all electrons are referred to a common center, usually the center of mass of the molecule. Such variety of approximations (which are needed to deal with molecular systems), together with the choice of basis functions or adopted numerical approach, translates into a considerable non uniformity in the quality of the end product. Except for $H_2$, for most molecules the PI cross sections obtained using different theoretical or numerical methods show no overall satisfactory agreement, on the one hand between them and, on the other hand, with experimental data. This is illustrated below with four molecules: $H_2$, $N_2$, $CO_2$, and $C_6H_6$. We emphasize that almost all experimental data presented here have no explicit error bars, either because they are not indicated in the given references or because they are too small, typically smaller than 3%.

## 3.1 $H_2$

We start with $H_2$, the simplest many-electron molecule. Figure 1 shows the PI cross sections obtained using different methods: self-consistent field (SCF,

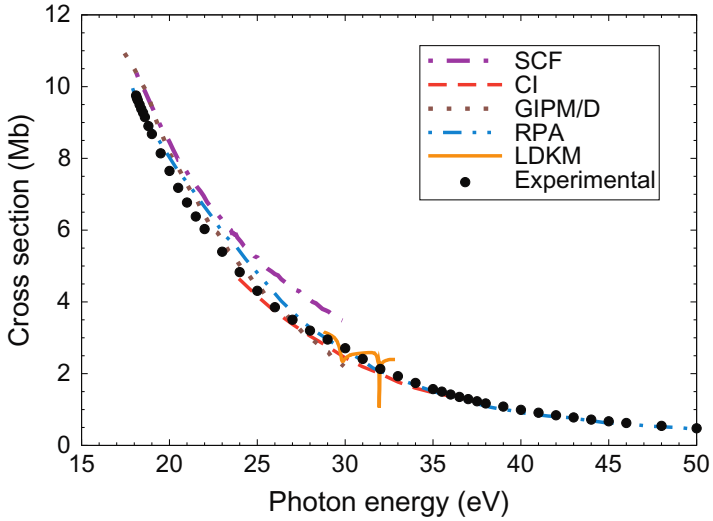


**Figure 1** PI cross section in Mb versus photon energy in eV for the ground state of $H_2$ molecule. We compare the results obtained using SCF[33] (purple (dark gray in the print version), dash-dot); CI[34] (red (gray in the print version), dash); GIPM/D[35] (brown (gray in the print version), dots); RPA[36] (blue (gray in the print version), dash-dot-dot), and LDKM[37] (orange (light gray in the print version), solid) with experimental data[32] (black dots).

see Section 4.2.1), configuration interaction (CI, see Section 4.1), ground state inversion method (GIPM/D, see Section 4.7.2), random-phase approximation (RPA, see Section 4.9) and logarithmic derivative Kohn method (LDKM, see Section 4.11.1). They are further compared with the experimental data of Chung et al.[32] For this example, SCF and CI calculations used OCE, and LDKM the FC approximation. Except for the SCF results, we see an excellent agreement between all theories with experimental data. Indeed, the molecule $H_2$ is sufficiently simple to allow for a PI study taking into account all interactions. One aspect, though, that remains challenging is to calculate precisely the positions and widths of the doubly excited states that depend on the nuclear motion.

## 3.2 $N_2$

We show in Fig. 2 the PI cross sections for the outer valence orbital $3\sigma_g$ of $N_2$. For such MO, we show calculations performed with CI (Section 4.1), time-dependent density functional theory (TD-DFT, see Section 4.3.2), multiple-scattering X$\alpha$ (MS X$\alpha$, see Section 4.6), Stieltjes–Tchebycheff technique (STT, see Section 4.10) and iterative-Schwinger method (ISM, see Section 4.12.1). Note that the results for CI and TD-DFT were obtained using OCE, and for ISM using the FC approximation. The theoretical cross sections are compared with the experimental results of Plummer et al.[38]

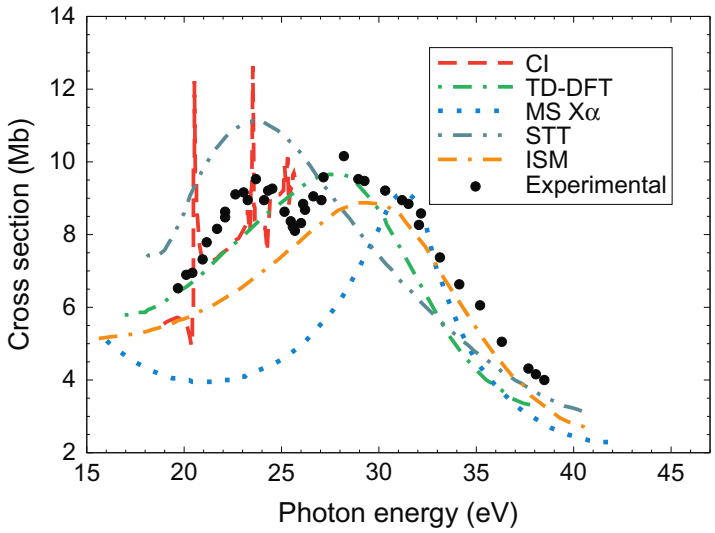


**Figure 2** Partial PI cross section in Mb versus photon energy in eV from the MO $3\sigma_g$ of $N_2$. Results for CI[39] (red (dark gray in the print version), dash); TD-DFT[40] (green (gray in the print version), dash-dot); MS X$\alpha$[41] (blue (dark gray in the print version), dots); STT[42] (gray, dash-dot-dot), and ISM[43] (orange (light gray in the print version), dash-dash-dot) are compared with experimental data[38] (black dots).

The situation changes drastically when moving from $H_2$ to a more complex molecule such as $N_2$. The figures show that the agreement between different theories and experimental data is basically lost, especially for energies close to the threshold. Moreover, only a partial agreement for higher energies is observed. Except for the CI results, none of the other calculations reproduces the different series of resonances located between 20 and 25 eV.

## 3.3 $CO_2$

The PI cross sections for $CO_2$ are shown in Fig. 3 for the MO $1\pi_g$. We compare the results obtained with GIPM/D (Section 4.7.2), STT (Section 4.10), ISM (Section 4.12.1) and *R*-matrix method (RMM, see Section 4.8). The experimental data are taken from Brion and Tan.[44]

Here, results for ISM and RMM used both the FC and the FN approximations. Depending on the energy range, the different theoretical calculations present again only a partial agreement, and even if they cannot reproduce completely the experimental data, they perform rather well beyond 25 eV. Although the center of mass of $CO_2$ is close to the C atom because of its linear geometry, this molecule is particularly difficult to describe: the density of charge is completely delocalized around the molecule and only the use of multicenter wavefunctions yields acceptable PI results, as in the GIPM/D case.

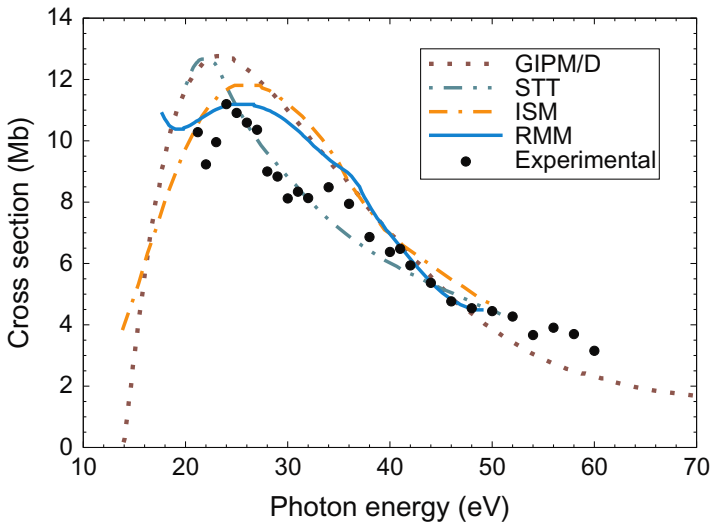


**Figure 3** Partial PI cross section in Mb versus photon energy in eV from the MO $1\pi_g$ of $CO_2$. Results for GIPM/D[45] (brown (dark gray in the print version), dots); STT[42] (gray, dash-dot-dot); ISM[46] (orange (light gray in the print version), dash-dash-dot), and RMM[47] (blue (dark gray in the print version), solid) are compared with experimental data[44] (black dots).

### 3.4 $C_6H_6$

Finally, for benzene ($C_6H_6$), PI cross sections for the outer valence orbital $1e_{1g}$ are shown in Fig. 4. The theoretical results obtained using DFT (Section 4.3.1), TD-DFT (Section 4.3.2), GIPM/D (Section 4.7.2) and LDKM (Section 4.11.1) are compared with the experimental data of Carlson et al.[48]

This is a rather complex molecule to describe theoretically and the difficulties show up in the PI spectra. None of the calculations accurately reproduce the resonances (neither their energy position nor their intensity), let alone the overall cross section magnitude except at rather high photoelectron energies.

As evidenced from Figs. 1 to 4, except for $H_2$, for all other molecules we can draw similar conclusions: (1) major disagreement between methods are clearly seen when comparing PI cross sections; (2) experimental data (in particular near threshold) are generally not well reproduced (other features of the continuum spectra are also difficult to reproduce). This is also true for $H_2O$, $NH_3$ or $CH_4$ molecules; the cross sections will be presented in Section 5.3, where we shall compare different theoretical calculations including ours obtained with the Sturmian approach. To have an overview of most methods that have been proposed to describe molecular PI, we present in the next section a survey and indicate to which molecules they have been applied (a rather complete list is presented in Appendix).

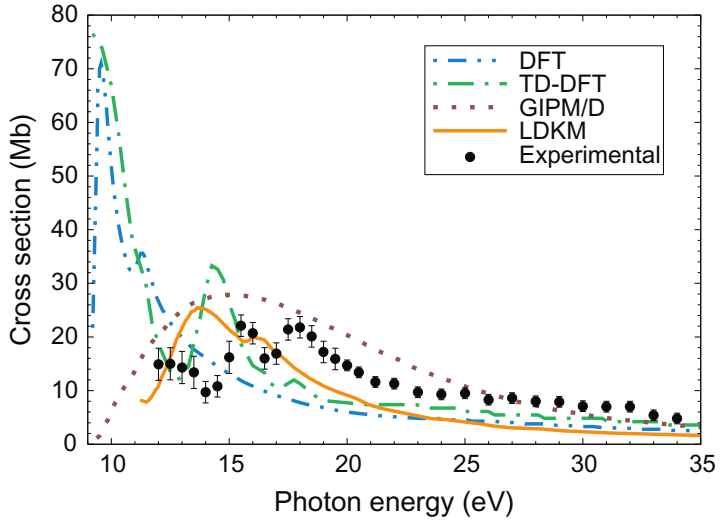


**Figure 4** Partial PI cross section in Mb versus photon energy in eV from the MO $1e_{1g}$ of $C_6H_6$ (benzene). Results for DFT[49] (blue (dark gray in the print version), dash-dot-dot); TD-DFT[50] (green (gray in the print version), dash-dot); GIPM/D[51] (brown (dark gray in the print version), dots), and LDKM[52] (orange (gray in the print version), solid) are compared with experimental data[48] (black dots).

# 4. SURVEY OF THEORETICAL METHODS

## 4.1 CI

One of the "classical" methods used to study electronic structure in atoms and molecules is configuration interaction (CI); a description of its use for the study of PI of molecules can be found in Ref. 53.

Some results obtained using the CI method are the studies by Daasch et al.[54] for $CO_2$, van Dishoeck et al.[55] for HCl and Decleva et al.[56] for $O_3$. Using B-splines[57] as a basis set, Apalategui and Saenz[58] studied multiphoton ionization of $H_2$; Vanne and Saenz[59] studied $HeH^+$; Fojón et al.[60] also studied $H_2$; Sanz–Vicario et al.[34] studied PI of $H_2$ by ultrashort laser pulses and Sansone et al.[28] for $H_2$ and $D_2$; Dowek et al.[61] studied circular dichroism in $H_2$. Using the so-called time-dependent CI,[62] we find the work of Klinkusch et al.[63] for LiCN, and of Sonk and Schlegel[64] for $C_4H_6$ (butadiene). Finally, using the multichannel CI complete-active-space,[65] we can find the work of Stratmann et al.[39] for $N_2$, and of Stratmann and Lucchese[66] for $O_2$.

## 4.2 Hartree–Fock Methods

### 4.2.1 Self-Consistent Field

Among the studies that have used the Hartree–Fock (HF) method and the self-consistent field (SCF) to study PI of molecules, we find the work of Dalgarno[67] for $CH_4$; Kelly[33] studied $H_2$; Schirmer et al.,[68] together with the Green's function formalism, studied the inner-valence PI of $N_2$ and CO; Padial et al.,[1] using Gaussian-type orbitals (GTOs), studied $C_2$. For calculations performed with the relaxed-core HF approximation, we have the results of Larkins and Richards[69] for $Li_2$; the studies of Saito et al. on the *K*- shell photoelectron angular distribution from $CO_2$[70] and from $NO_2$[71]; Semenov et al.[72] studied the PI from the *K*-shell of CO. We should also mention the review of different applications of the SCF by Ågren et al.[73]

### 4.2.2 Multiconfiguration Time-Dependent Hartree–Fock

In general, it is difficult to describe with high precision highly excited states and nonadiabatic dynamics in molecules, especially if one is interested in studying ionization by high-intensity radiation fields. The multiconfiguration time-dependent Hartree–Fock (MCTDHF) approach is a method that uses a linear combination of determinants of time-dependent orbitals, and is flexible enough to describe the response of a molecule to short and intense laser pulses. The formalism can be found in Refs. 74–76.

The MCTDHF has been used by Kato and Kono[76] and by Haxton et al.[77] to study PI of $H_2$ by intense laser fields, and also by Haxton et al.[78] for HF.

## 4.3 Density Functional Theory

Density functional theory (DFT) is widely used in quantum chemistry. It allows for easy determination of the electronic structure for given systems (an atom, a molecule, a crystal, etc.), regardless of its extension or the number of particles that constitute it. While "standard" quantum mechanics works directly with the many-body wavefunctions of the different particles in a given system, DFT uses the one-electron electronic density $n(\mathbf{r})$ and is based on two theorems, called the Hohenberg–Kohn theorems.[79]. In different implementations of the DFT to study PI of molecules, $n(\mathbf{r})$ is calculated using a conventional linear combination of AOs (LCAO).[49]

### 4.3.1 Kohn–Sham DFT

In the Kohn–Sham DFT (KS DFT),[80] the Hamiltonian of the molecular system is determined by the density of the occupied orbitals in the ground state and in terms of the Hartree potential, the electron–nuclei interaction, and the so-called exchange-correlation potential which contains all the "unknowns" of the system. Different potentials are available in the literature for different atomic and molecular systems (see, for instance Refs. 81 and 82), based, for example, on the local density approximation or on the generalized gradient approximation.

The KS DFT has been used by Venuti et al.[49] to study PI in $C_6H_6$; by Stener and Decleva, using the OCE approximation, to study HF, HCl, $H_2O$, $H_2S$, $NH_3$, and $PH_3$ (Ref. 83), and $CH_4$, $SiH_4$, $BH_3$, and $AlH_3$ (Ref. 84). Toffoli et al.,[85] using the multicenter expansion, calculated cross sections for $Cl_2$, $(CO)_2$, and $Cr(CO)_6$. Woon and Park[86] also studied $C_6H_6$ (benzene), $C_{10}H_8$ (naphthalene), $C_{14}H_{10}$ (anthracene) and $C_{16}H_{10}$ (pyrene). Stranges et al.[87] studied the dynamics in circular dichroism of the $C_3H_6O$ (methyl-oxirane). Toffoli et al.[88] studied the PI dynamics in $C_4H_4N_2O_2$ (uracil).

### 4.3.2 Time-Dependent DFT

Time-dependent DFT (TD-DFT)[89] constitutes another line of development of the DFT methods. In the first order time-dependent perturbative scheme, where the zeroth order is equivalent to the KS DFT,[90] the linear

response of the electronic density $n(\mathbf{r})$ to an external weak time-dependent electromagnetic field can be described by a SCF potential, given by Zangwill and Soven.[91]

The TD-DFT has been used by Levine and Soven[40] to calculate photoemission cross sections and asymmetry parameters of $N_2$ and $C_2H_2$. Stener, Decleva and coworkers, using B-splines[57] and the OCE, studied PI for different molecules: Stener and Decleva[90] calculated the cross sections for $N_2$ and $PH_3$; Stener et al.[92] for $CH_4$, $NH_3$, $H_2O$, and HF; Stener et al.[93] for CO and also from the *K*-shell[94]; Fronzoni et al.[95] for $C_2H_2$; Stener et al.[50] for $CS_2$ and $C_6H_6$; Toffoli et al.[96] and Patanen et al.[97] for $CF_4$, and Holland et al.[98] for pyrimidine and pyrazine. We also find the work of Russakoff et al.[99] for $C_2H_2$ and $C_2H_4$, and by Madjet et al.[100] for $C_{60}$. Different results for molecular PI have been reviewed by Stener et al.[101]

For the sake of completeness, we also mention some studies of molecular PI that use a slightly different approach, the static-exchange DFT: Plésiat et al.[102] investigated PI of $N_2$ and CO, and Kukk et al.[103] from the inner-shells of CO.

## 4.4 Complex Methods

### 4.4.1 Complex Scaling

The complex scaling (CS) method[104–105] has been used extensively to study ionization and, mainly, resonance phenomena in atoms and molecules. The idea behind this method is to scale the coordinates of all particles in the Hamiltonian by a complex-valued scale factor: $r \rightarrow re^{i\theta}$. One variant of the CS is the so-called exterior complex scaling (ECS),[106–108] whereby the coordinates scale only outside a fixed radius $R_0$

$$r \rightarrow R(r) = \begin{cases} r & \text{for } r \leq R_0, \\ R_0 + (r - R_0)e^{i\theta} & \text{for } r > R_0. \end{cases} \tag{7}$$

The ECS method has been applied to study general scattering problems using $L^2$ basis set representations. It is especially well suited to study ionization processes in molecules, since the definition of the exterior scaling (7) avoids complicated scaling expressions in the nuclear attraction terms of the Hamiltonian[107] when $R_0$ is large enough to enclose all the molecular nuclei.

The ECS has been used mainly by McCurdy, Rescigno, Martín and coworkers to study different ionization processes in atoms and molecules: McCurdy and Rescigno[109–110] used Cartesian Gaussian-type orbitals (CGTOs) to calculate PI cross sections of $H_2^+$; Vanroose et al.,[111–112] using

B-splines,[57] studied double PI (DPI) of $H_2$; Rescigno et al.[113] performed *ab initio* DPI calculations of $H_2$; Tao et al., using discrete variable representation (DVR),[114] calculated PI cross sections for $H_2^+$ [115–116] and angular distribution for DPI of $H_2$.[117]

### 4.4.2 Complex Basis Functions

In the complex basis function (CBF) technique[109,110,118] (the CS method can be considered a particular case of the CBF where the basis functions are defined in terms of the physics of the problem), the continuum scattering information is extracted from a finite-matrix representation of the electronic Hamiltonian in a set of complex square-integrable basis functions. The resulting matrix elements necessary to obtain the cross section, can be calculated efficiently using a discrete basis set approximation to the spectrum of the Hamiltonian.[109]

The CBF technique, together with complex GTO, has been used by McCurdy and Rescigno[109] to calculate PI cross section of $H_2^+$; by Yu et al.[118] for valence- and *K*-shell ionization of $N_2$, and by Morita and Yabushita[119] for $H_2^+$ and $H_2$.

## 4.5 Linear Algebraic Method

The linear algebraic method (LAM), developed by Collins and Schneider,[120–121] has been applied successfully to study molecular excitation and ionization by electron collisions. The adaptation of the method to study PI in molecules is given in Ref. 122. The LAM presents the advantage of including explicitly an effective optical potential in order to introduce correlation effects into the scattering solution.[122]

While the initial state is treated separately, usually in terms of GTO or CGTO,[120] the method is used to calculate directly the ejected electron unbound wavefunction that satisfies the TISE. To do so, the configuration space is divided into two regions, with the boundary at $r = a$: (1) for $r \geq a$, where nonlocal effects are negligible, the wavefunction can be calculated by standard propagation procedures; (2) for $r < a$, where exchange and correlation effects are important, the wavefunction is expanded in two terms: one as a linear combination of the wavefunctions of the molecular-ion target and the scattering wavefunction, and the other in a set of "correlation" functions that are added for completeness.[122]

In the LAM, one obtains a set of differential equations in the SEA, that can be converted into a set of radial integro-differential equations using an

expansion in partial waves of the electronic wavefunctions. Then, this set of scattering equations is further transformed into a set of coupled integral equations using Coulomb Green's functions.[120] Finally, by introducing a discrete quadrature to evaluate the integrals, one obtains a set of linear-algebraic equations that can be solved with standard linear systems routines. This solution must be matched at $r=a$ with the result of the propagation scheme to the asymptotic region. More details on the effective optical potential are given in the Refs. 120, 122 and 123.

To our knowledge, this method has been used only by Collins and Schneider[122] to calculate cross sections for $H_2$, $N_2$, NO, and $CO_2$.

## 4.6 Multi-Scattering

The multiple-scattering method (MSM) has been developed in different physics fields, as in nuclear physics,[124] solid state physics,[125] and also in atomic and molecular physics (see, for example, Refs. 126 and 127, and references therein). The idea behind the MSM is to represent the molecular field, that in general is highly noncentral in the molecular core region, by a set of three potentials $V_{\mathrm{I}}$, $V_{\mathrm{II}}$, and $V_{\mathrm{III}}$, defined in different nonoverlapping spheres (called muffin-tin partitioning): (I) defined by the $\{\mathrm{I}_i\}$ spherical regions containing the different atomic nuclei at their center $r_i=0$, and with radii $\{\rho_i\}$; (II) defined by $r_i>\rho_i$ and $r_0<\rho_{\mathrm{III}}$, where $r_0$ is the radial coordinate from the center of the molecule and $\rho_{\mathrm{III}}$ is the outer sphere radius, measured from the molecular center. In general, the potential $V_{\mathrm{II}}$ is considered constant; (III) defined by $r_0\geq\rho_{\mathrm{III}}$. The potential $V_{\mathrm{III}}$ has a spherical symmetry. One can construct the photoelectron continuum wavefunction taking into account the continuity conditions between all three regions, and imposing the incoming boundary conditions (3) in the external region. The total wavefunction is written as $\Psi=\sum_i\Psi_i+\Psi_{\mathrm{II}}+\Psi_{\mathrm{III}}$, where each term is a solution to the potential of the corresponding region of the molecular field, and obeys the adequate asymptotic boundary conditions.

The MSM or, equivalently, multiple-scattering with an undetermined factor $\alpha$ (MS X$\alpha$),[128] have been widely used to study ionization of molecules by photon and electron impact. For example, Davenport calculated cross sections for $N_2$ and CO,[41,129] and for $H_2$[129]; Dehmer and Dill calculated the $K$-shell PI of $N_2$[130]; Grimm[131] calculated the cross section for $C_2H_4$ and Grimm et al.[132] for $N_2$, CO, $CO_2$, COS, and $CS_2$; Rosi et al.[133] studied PI in $CH_4$ and $CF_4$; Tse et al.[134] investigated the photoabsorption spectra in $SiCl_4$; Ishikawa et al.[135] studied, implementing a DVR[114] method, $SiH_4$,

$SiF_4$, and $SiCl_4$; Powis studied PI in $PF_3$[136], $CH_3I$[137], and $CF_3Cl$.[138] Finally, Jürgensen and Cavell[139] compared directly experimental results with the MS X$\alpha$ for $NF_3$ and $PF_3$.

## 4.7 Plane-Wave-Based Methods

### 4.7.1 Plane-Wave and Orthogonalized Plane-Wave Approximations

The simplest description of an ionized electron is the plane-wave approximation (PWA), but it is not expected to give accurate results near threshold.[140] To our knowledge, the first implementations of the PWA are due to Kaplan and Markin,[141–142] Lohr and Robin,[143] and to Thiel and Schweig.[144–145]

The final state of the molecule describes one electron that has been excited from a given initial MO to a continuum normalized plane-wave orbital.[140] This plane-wave is not necessarily orthogonal to any of the occupied MOs; if orthonormality is imposed, we have the orthogonalized PWA.

The PWA and the orthogonalized PWA, together with Slater-type orbitals (STOs) to describe AO, have been used by Rabalais et al.[146] and by Dewar et al.[147] to calculate PI cross sections for $H_2$, $CH_4$, $N_2$, CO, $H_2O$, $H_2S$, and $H_2CCH_2$. Huang et al.[148] used the orthogonalized PWA to calculate angular asymmetry parameters for $H_2$, $N_2$, and $CH_4$. Beerlage and Feil[149] calculated cross sections for HF, $(CN)_2$, CaHCN, $C_2(CN)_2$, $N_2$, CO, $H_2O$, furan, pyrole and tetrafluoro-pyrimidine. Schweig and Thiel[150] calculated the relative band intensity of $N_2$, CO, $H_2O$, $H_2S$, $NH_3$, $PH_3$, $CH_4$, $(CH_3)_2S$, $C_6F_6$, among others. Hilton et al.[151] have used the so-called effective PWA to calculate cross sections for $H_2$, CO, $H_2O$, and $C_2H_4$. Finally, Deleuze et al.[152] used the orthogonalized PWA, together with a many-body Green's function framework, to calculate PI cross sections for $CH_4$, $H_2O$, $C_2H_2$, $N_2$, and CO.

### 4.7.2 Ground Inversion Potential Method

The so-called ground state inversion potential method (GIPM) has been developed by Hilton, Hush, Nordholm and coworkers[151,153] with the aim of obtaining a chemical theory of PI intensities.[154] This method uses the standard one-electron PWA, the orthogonalized PWA or the energy shifted PWA[151] in order to calculate the electronic continuum final wavefunction. The cross section is obtained from an atomic summation theory together with a plane wave analysis of diffraction effects from photoelectron amplitudes from different atoms that interfere with each other.[35,154] The main difference of GIPM with a standard PWA is that the potential felt by an electron

when leaving an atomic center in a molecule is calculated directly by inversion of the ground state HF orbital.[153–154] The GIPM theory can include three important effects: change in the atomic orbitals nature upon formation of the molecule, diffraction effects[154] and exchange in an exact sense.

The GIPM has been used by Hilton et al. to calculate PI cross sections for $H_2O$[155] and for $H_2$, $N_2$, and CO.[35] Also Kilcoyne et al. calculated cross sections for $H_2$, HF, and $N_2$[154]; H2O, $NH_3$, and $CH_4$[156]; CO, $CO_2$, and $N_2O$,[45] and for $C_2H_4$ and $C_6H_6$.[51]

## 4.8 *R*-Matrix Method

Originally introduced in nuclear physics, the *R*-matrix method (RMM) has been adapted to atomic and molecular physics by Burke and coworkers (see Ref. 157 and references therein). Applications of this method, in particular for electron collisions, have been reviewed elsewhere.[158–160] The idea behind the RMM is to enclose the scattering particles and the target within a sphere of radius *a*, so that it should be possible to characterize the system using the eigenenergies and the eigenstates computed within the sphere. Then by matching them to the known asymptotic solutions, one can extract all the scattering parameters. The *R*-matrix is defined as the matrix that connects the two regions in which the space is divided into. They are: (1) an internal region, where all the particles are close to one another, so that the short-range interactions and exchange are important; (2) an external region, where all particles are still interacting, but the forces are direct and could have a multipolar character. In the most conventional use of the RMM, the Hamiltonian of the internal region is diagonalized in order to obtain the *R*-matrix eigenenergies and eigenfunctions, generally using the nonadiabatic formalism.[161] The initial and final states are expanded in terms of these eigenstates. The corresponding coefficients for the initial state are usually obtained by performing an all-channels-closed scattering calculation, and in this case the problem is reduced to find the zeros of a determinant.[162–163] To obtain the coefficients for the final state, calculations of electron scattering by the corresponding molecule can be made and the resulting *R* matrices represent the result of a full nonadiabatic treatment of the internal region of the scattering problem,[160] and provides the solution in the external region.[164] Finally, with both sets of coefficients, it is possible to calculate the required transition dipole moments, and thus the PI cross section (4).

Since the corresponding formalism is relatively new, the RMM has not been used for molecules as much as for atoms. However, we have the works

by Tennyson et al.[165] for $H_2$, and by Tennyson[166] for $H_2$ and $D_2$. The so-called *R*-matrix Floquet theory[167–168] has been used by Burke et al.[168] and by Colgan et al.[169] to study multiphoton processes in $H_2$. Saenz,[170] using STOs, studied PI in $HeH^+$. Tashiro[171] calculated cross sections for $N_2$ and NO. Finally, Harvey et al.[47] recently studied $CO_2$, using GTOs combined with Coulomb and Bessel functions.

## 4.9 Random Phase Approximation

The random phase approximation (RPA) is a method that has been applied with success to study PI in atoms and molecules.[172–173] One advantage is that PI cross sections calculated in length or velocity gauges coincide. Additionally, the computational effort required in the RPA implementation is comparable to calculations in the single active electron (SAE) approximation, since the RPA uses only two-electron integrals involving two occupied and two unoccupied orbitals.[174–175]

In the standard procedure of the RPA, the ground state and the one-electron wavefunctions for the excited and continuum states of the molecule are calculated at HF level. With these, all required matrix elements and in particular the Coulomb and dipole matrix elements, can be calculated directly. Next, the RPA dipole matrix elements are calculated solving the corresponding equation, and the results are used to obtain directly PI cross sections or the required observables.[174–177]

The RPA has been used to study PI of $H_2$ by Martin et al.,[36] by Schirmer and Mertins[178] and by Semenov and Cherepkov.[177,179] For $N_2$, we can find calculations performed by Lucchese and Zurales[180]; by Semenov and Cherepkov[176,181]; by Yabushita et al.,[175] using complex functions; and by Montuoro and Moccia,[182] using mixed $L^2$ basis sets (STOs and B-splines[57]). For $H_2S$, we have the results of Cacelli et al.[183] For LiH, calculations were performed by Carmona-Novillo et al.[184] For $C_2H_2$, we have the results of Yasuike and Yabushita,[185] who used complex basis functions (see Section 4.4.2) and by Montuoro and Moccia, using the mixed $L^2$ basis sets. We can find also calculations for the *K* shell of $N_2$ by Cherepkov et al.[186]; for the ion $C_{60}^+$ by Polozkov et al.,[187] or for the fullerenes $C_{20}$ and $C_{60}$ by Ivanov et al.[188] Extensive calculations have been performed by Cacelli et al.,[189] to study PI in $CH_4$, $NH_3$, $H_2O$ and HF, and by Amusia et al.,[172] who used the RPA with exchange to calculate PI cross sections of $CH_4$, $C_2H_6$, $C_3H_8$, $C_2H_4$, $C_2H_2$, $NH_3$, $H_2O$, $CN^-$, $N_2$, CO, $CO_2$, $N_2O$, and $NO_2^-$.

## 4.10 Stieltjes–Tchebycheff Technique

The Stieltjes–Tchebycheff technique (STT), developed by Langhoff and coworkers (see, for example, Ref. 190 and 191 and references therein), is based on theorems from the theory of moments[192]; its flexibility allows the use of different type of basis sets.[191,193,194] The technique has been widely and successfully used to study ionization processes in different atomic and molecular systems.

The strength of the interaction of unpolarized radiation with a target gas can be described by Kramers–Heisenberg expression of the polarizability (frequency dependent) of the constituent molecules. This strength can be written as a Stieltjes integral over the appropriate oscillator strength distribution[190,194] or, alternatively, by the use of the cumulative oscillator-strength distribution which can be approximated by an histogram (Stieltjes procedure). Even if such an histogram cannot represent adequately the continuum of the molecule, it can give good approximations to the related power moments, and it rigorously bounds the correct distribution through Tchebycheff inequalities.[192] Technical details about the direct computational implementation of the STT are provided in Ref. 191.

The STT has been used to study PI in CH, using STOs, by Barsuhn and Nesbet[195]; in $H_2$, using GTOs in a CI method (see Section 4.1), by ONeil and Reinhardt[196]; in $N_2$, together with GTOs, by Rescigno et al.[194] and using LCAO with optimized STOs by Stener et al.[42] In $H_2O$ by Williams et al.[197] and by Delaney et al.[198] in the SEA, both using GTOs; by Diercksen et al.,[199] using Cartesian Gaussian basis sets and by Cacelli et al.[200] using STOs in the independent-channel approximation. By Cacelli et al., we also find calculations for $NH_3$,[200] HF,[201] HCl,[202] $H_2S$,[203] and $CH_4$.[201] For CO, we mention the work by Görling and Rösch,[204] who used GTOs. For $F_2$, Orel et al.[205] used contracted Gaussians. For $C_6H_6$, Gokhberg et al.[206] used the STT together with the Lanczos algorithm. Finally, Stener et al.[42] have performed calculations using LCAO with optimized STOs for $CO_2$, $N_2O$, $SF_6$, $C_2N_2$, $TiCl_4$, and $Cr(CO)_6$.

## 4.11 The Kohn Variational Method

Among different approximate methods used to determine the energy spectra and the corresponding wavefunctions, we have the perturbation theory and the standard Ritz variational method,[26] where approximate solutions of the TDSE or the TISE for a given problem are found in a subspace of the real problem. Besides the standard Ritz method, there is also, e.g., the Kohn

variational method (KVM).[207] The idea behind the latter is to find a variational expression that allows one to calculate the wavefunction with a correct asymptotic behavior. This is dictated by two arbitrary $f_\ell(r)$ and $g_\ell(r)$ functions, that behave asymptotically as the regular $F_\ell(kr)$ and, respectively, irregular $G_\ell(kr)$ Coulomb functions. The trial wavefunction can be written as

$$\psi_\ell^{\mathrm{t}}(r) = f_\ell(r) + \lambda^{\mathrm{t}} g_\ell(r) + \sum_i c_i \varphi_i(r), \tag{8}$$

where $\{\varphi_i\}$ is a set of $L^2$ functions and $\lambda^{\mathrm{t}}$ is a trial parameter. The Kato identity[208] is used to find a stationary $\lambda^{\mathrm{s}}$ value. We can distinguish two options for the trial wavefunction (8): (1) if $f_\ell$ and $g_\ell$ are the regular and irregular Coulomb functions, then we have $\lambda = \tan\delta_\ell$, where $\delta_\ell$ is the phase shift related to a short range potential; (2) if $g_\ell$ is an outgoing function $h_\ell^{(-)}$, called "regularized" irregular Coulomb function (defined as $h_\ell^{(-)}(r) = ik^{-1/2}[F_\ell(kr) - ic(r)G_\ell(kr)]$, where $c(r)$ is a cutoff function) then $\lambda = \mathrm{e}^{i\delta_\ell}\sin\delta_\ell$, i.e., the $T$-matrix (transition matrix). In this case, we have the complex Kohn method.[208–209]

Two different implementations of the KVM in the study of PI of molecules are separately hereafter described.

### 4.11.1 Logarithmic Derivative Kohn Method

The logarithmic derivative Kohn method (LDKM),[210–211] and its variant, the finite-volume variational method,[212] were originally proposed to generate a translational basis for reactive scattering, using Lobatto shape functions.[211,213,214] In this method, all the required radial integrals are performed explicitly over a finite volume $V$, usually a sphere. The main difference between the LDKM and the standard KVM is that different coefficients are added to the functions $f_\ell$ and $g_\ell$ in (8); these coefficients can be determined by matching the wavefunction and their derivatives with the exact Coulomb functions across the surface that delimits the integration volume $V$.[52,214] In many of the implementations of the LDKM, Lobatto shape functions, referred usually as free-type functions, are used as the basis set $\{\varphi_i\}$ in (8).

The LDKM has been used to calculate PI cross sections for $H_2^+$ by Le Rouzo and Raşeev[212] and by Rösch and Wilhelmy[214]; Raşeev[37] studied autoionization in $H_2$; and Wilhelmy et al.[52,215] calculated cross sections and asymmetry parameters for $N_2$, CO, and $C_6H_6$.

### 4.11.2 Complex Kohn Method

The complex Kohn method (CKM), developed by McCurdy, Rescigno and coworkers to study excitation and ionization of molecules by electron collisions,[209,216,217] have proved to be very effective, in particular in the first-order calculation of dipolar transition moments.[216] The adaptation of the method to study PI in molecules has been described by Lynch and Schneider.[218] Different elections of the arbitrary cutoff function $c(r)$ or the irregular function $g_\ell(r)$ have been tested.[218–219]

The CKM has been used Lynch and Schneider[218] to study PI of $H_2$ and $N_2$; by Rescigno et al.[220] to study CO, examining the effects of the inter-channel coupling; Orel and Rescigno[221] to study $NH_3$ and, more recently, Jose et al.[222] to study PI of $SF_6$ also adding inter-channel coupling effects.

## 4.12 The Schwinger Variational Method

While many variational methods are based on the TISE (a differential equation), several others, as the Schwinger variational method (SVM)[223] are based on the equivalent integral equation, the Lippmann–Schwinger equation (LSE).[224–225]

The advantage of the LSE over the TISE to study collisions processes is that the correct boundary conditions of the problem are automatically incorporated through the use of the corresponding Green function $G^C$. The SVM is a powerful formulation of the scattering problem that can provide highly accurate solutions without requiring expansions in very large basis sets.[226–227] The idea behind this method is to obtain a stationary variational condition over the $T$-matrix. In general, one can obtain better converged results using the SVM compared to the KVM results.

The implementation of the SVM has been developed along two methods, named the Schwinger multichannel method[228] and the iterative-Schwinger method (ISM). The latter, and a variant using continued fractions, are now briefly described.

### 4.12.1 Iterative Schwinger

The ISM is an iterative approach to the solution of collisions problems using the SVM[226] to solve the LSE. The first implementation of ISM[227,229,230] was the study of scattering of low-energy electrons by atoms and molecules. In the case of molecules, the fixed-nuclei approximation was used together with the assumption that the interaction between the ionized electron and the molecular ion is described by the static-exchange potential.[230–231] The

description of the ISM implementation to study PI is given with details in Refs. 43 and 46.

In the ISM instead of solving the associated LSE for each partial-wave of the scattering function, one solves equivalently a LSE for the $T$ matrix[226,231]: $T = U + UG^{C}T$. The iterative method begins by approximating the short-range potential $U$ by a separable potential $\tilde{U}$, using an initial set of expansion functions $R$; then the scattering solutions for the approximate potential $\tilde{U}$ are obtained from the corresponding LSE. The iterative procedure is continued by augmenting the original set of functions with those obtained with the approximated potential. Using this augmented set of functions, the first iteration is completed by calculating a new $T$ matrix. A second iteration is begun by constructing a new set of solutions and combining them with the initial trial functions set; this will yield a new $T$ matrix. The iterative procedure is continued until the wavefunctions converge, yielding the LSE solutions for the exact potential $U$.[230–231]

This method has been widely used to study PI of molecular systems. Using CGTO as the initial set of functions $R$, we find calculations by Lucchese et al.[43] for $N_2$; using spherical GTOs, Lucchese et al.[46] calculated PI cross section for $CO_2$ and Lynch et al.[232] for $C_2H_2$. Natalense et al. presented results for $SF_6$[233] and for $CH_4$, $CF_4$, and $CCl_4$[234]; Machado et al. for $H_2O$[235] and $SiH_4$[236]; Machado and Masili[237] studied $H_2$; Stephens and McKoy[238] for OH; Braunstein et al.[239] for $CH_4$; Wells and Lucchese[240] for $C_2H_2$; for $C_{60}$ we find the results by Gianturco and Lucchese[241]; and Wiedmann et al.[242] calculated the rotationally resolved PI cross section for $CH_3$, $H_2O$, $H_2S$, and $H_2CO$.

### 4.12.2 Continued Fractions

The method of continued fractions (MCF) was originally proposed by Horáček et Sasakawa[243–244] for the study of elastic scattering of fast electrons by atoms; subsequently, Lee et al. adapted it to study scattering of slow electrons by atoms[245] and by linear molecules,[246] and extended it to study ionization by electron collisions in polyatomic molecules.[247–248] The extension of the MCF to the PI study of molecules is explained with details in Ref. 249. The idea is to represent the scattering matrix as a continued fraction. The continuum wavefunction is obtained from the solution of the LSE using the static-exchange potential, with the long-range Coulomb potential of the ionic core removed. The MCF does not require basis functions and it is characterized by rapid convergence.

The application of the MCF starts with the definition of a $n$th-order weakened potential operator $U^{(n)}$, from which the reactance matrix **K** is expressed in the form of a continued fraction. The $n$th-order correction to **K**, as well as to the wavefunction, can be approximated successively. The operator $U^{(n)}$ becomes weaker and weaker as $n$ increases, and the procedure can be stopped after a few steps. The converged **K** matrix corresponds to the exact solution for a given potential $U$ in LSE.[249]

To our knowledge, the MCF has been used only to study PI of $NH_3$.[249]

### 4.13 Crank–Nicolson

The Crank–Nicolson (CN) method[250] was originally developed to solve differential equations of heat-conduction type numerically using a combination of backward/forward finite difference of all variables involved. It is correct up to the second order in $\hat{H}\Delta t$, and is numerically stable. The CN scheme can be used to propagate an initial wavefunction with an imaginary time evolution operator, in which, by the Wick rotation, the time $t$ is replaced by $-i\tau$. In such a way, any initial arbitrary state can converge directly to a particular desired state (bound or continuum), just by adjusting the time step of the propagator.

The CN scheme has been used to study general PI features by Goldberg and Shore[251]; we can find also different studies in PI of $H_2^+$ by Picón et al.,[252] Yuan et al.,[253] Silva et al.,[254] and Bian[255]. The ion $HeH^{2+}$ has been studied by Bian[255] and the angular distributions for $H_2$ by Yuan et al.[253]

## 5. STURMIAN APPROACH

### 5.1 Generalized Sturmian Functions

In the literature, we can find different approaches to Sturmian functions, depending on the type of problem to be solved. There are essentially two lines, one associated to bound states and another to scattering problems. The first line initiated by Shull and Löwdin,[256] has been formalized by Goscinski[257] and impulsed later on by Aquilanti and coworkers.[258–259] It is within this line that the generalized Sturmian functions were introduced by Avery and coworkers[260–261] to deal with many electron atoms and chemical systems. On the scattering line, the work was initiated by Rawitscher[262–263] and continued by Macek, Ovchinnikov and coworkers.[264–265] Some of us extended the scattering functions proposed by Rawitscher and started to use them in scattering studies with the name Generalized Sturmian Functions

(GSFs) to indicate that the basis functions are solving general atomic potentials.

Details on the GSF used here are given in Refs. 22 and 23 (and references therein) and only the essentials are recalled below. GSF are solutions of a Sturm–Liouville problem, from which Rotenberg[266–267] took the name. Noted $\mathcal{S}_n^{(\ell,\,E)}(r)$, they are regular at the origin and satisfy the two-body non-homogeneous Schrödinger equation

$$\left[-\frac{1}{2}\frac{\mathrm{d}^2}{\mathrm{d}r^2}+\frac{\ell(\ell+1)}{2r^2}+\mathcal{U}(r)-E\right]\mathcal{S}_n^{(\ell,\,E)}(r)=-\beta_n^{(\ell,\,E)}\mathcal{V}(r)\mathcal{S}_n^{(\ell,\,E)}(r), \quad (9)$$

where $E$ is an externally fixed parameter and $\beta_n^{(\ell,\,E)}$ are the eigenvalues for a given angular momentum $\ell$. In general, the generating potential $\mathcal{V}(r)$, a short-range potential, dictates the size of the inner region in which most of the dynamics is supposed to occur, while the auxiliary potential $\mathcal{U}(r)$ determines the common asymptotic behavior of all GSFs. This property is illustrated in Fig. 5, for functions with a fixed energy $E=0.5$ a.u., an auxiliary Coulomb potential with charge $Z=-1$ and a Yukawa generating potential. The outgoing asymptotic behavior of the GSFs with an auxiliary Coulomb potential is given by (see second term of (3))

$$\lim_{r\to\infty}\mathcal{S}_n^{(\ell,E)}(r)\propto \mathrm{e}^{-i\left(kr-\frac{Z}{k}\ln(2kr)-\ell\frac{\pi}{2}+\delta_\ell\right)}, \quad (10)$$

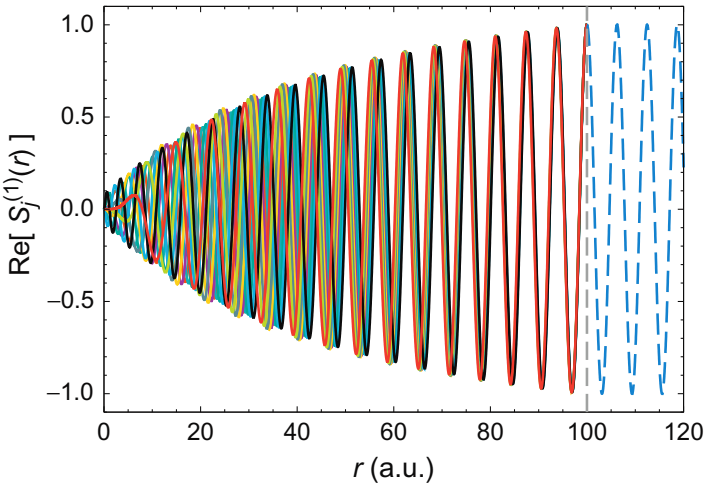


**Figure 5** Real part of 10 generalized Sturmian functions, with a fixed energy $E=0.50$ a.u. and $\ell=1$, obtained solving Eq. (9), for $r\in[0,100]$, together with a Coulomb auxiliary potential with charge $Z=-1$, and a Yukawa potential as a generating potential, with parameter $\alpha_{\text{short}}=0.0219$. The exact Coulomb (analytic) regular function (blue (gray in the print version), dash) is also shown.

where $\delta_\ell = \arg[\Gamma(1+1+\mathrm{i}Z/k)]$ is the Coulomb phase shift. Additionally, all the solutions form a complete basis set, with the potential-weighted orthogonality relation

$$\int_0^\infty \mathrm{d}r\, \mathcal{S}_{n'}^{(\ell,\,E)}(r)\mathcal{V}(r)\mathcal{S}_n^{(\ell,\,E)}(r) = \delta_{n'n}. \tag{11}$$

Note that the integral is defined without taking the complex conjugate of the function $\mathcal{S}_{n'}^{(\ell,\,E)}(r)$.

## 5.2 Sturmian Approach to Photoionization Process

We shall present in this section the theoretical formalism developed within a Sturmian approach for molecules. We start with a brief description of the molecular model potentials used, then we derive the driven equation of the TISE and provide the necessary formula to calculate the PI cross section. As a simple illustration of the numerical implementation in the atomic case, we show results for the hydrogen atom.

### 5.2.1 Molecular Model Potentials

To study PI of molecules, we shall use the SAE approximation[268] for the initial state wavefunction. We then need a molecular model potential that plays the role of a scattering potential. Consider the active electron placed in the MO $i$ of the ground state and denote $\phi_i(\mathbf{r})$ the corresponding wavefunction. The molecular model potential we shall use is the following[269]

$$V_{i\,\mathrm{mol}}(\mathbf{r},\mathbf{R}) = -\sum_{n=1}^{M}\frac{Z_n}{|\mathbf{r}-\mathbf{R}_n|} + \sum_{j=1}^{N_{\mathrm{MO}}} N_{ij}\int \mathrm{d}\mathbf{r}'\,\frac{\left|\phi_j(\mathbf{r}')\right|^2}{|\mathbf{r}-\mathbf{r}'|}, \tag{12}$$

where $M$ is the number of nuclei in the molecule, $Z_n$ is the charge of each nucleus, $\mathbf{R}_n$ is the position of each nucleus with respect to the molecule center of mass, $N_{\mathrm{MO}}$ is the number of MOs and $N_{ij} = 2 - \delta_{ij}$. This potential is the direct term within the SEA. For the sake of simplicity, the nuclei $\mathbf{R}_n$ dependence, collectively represented as $\mathbf{R}$, is omitted hereafter.

We shall take the MO $i$ given by Moccia; they are expressed as

$$\phi_i(\mathbf{r}) = \sum_{j=1}^{N} A_{ij}\mathcal{R}_j(r)S_{\ell_j}^{m_j}(\hat{r}), \tag{13}$$

where $S_{\ell_j}^{m_j}(\hat{r})$ are the real spherical harmonics,[31] and the $N$ radial wavefunctions are given as Slater type-orbitals (STOs)

$$\mathcal{R}_j(r) = \left[\frac{(2\zeta_j)^{2n_j+1}}{(2n_j)!}\right]^{1/2} r^{n_j-1}\mathrm{e}^{-\zeta_j r}, \tag{14}$$

with tabulated integers $n_j$ and exponents $\zeta_j$. These MOs allow one to calculate analytically, in a partial-wave expansion, the molecular model potential.

As mentioned before, in a typical experiment the molecules are randomly oriented. Although this is not the proper way to proceed, we may consider as starting point an angular average of the model potential (12), i.e., a central potential

$$U_{i\,\mathrm{mol}}(r) = \frac{1}{4\pi}\int_{4\pi} \mathrm{d}\hat{r}\; V_{i\,\mathrm{mol}}(\mathbf{r}). \tag{15}$$

This averaging procedure is illustrated through Fig. 6, where the effective charges $rU_{i\,\mathrm{mol}}(r)$ and $rV_{i\,\mathrm{mol}}(\mathbf{r})$ for two set of angles $(\theta,\phi)$ are compared in the case of $CH_4$. The effective charge goes from $-6$ at $r=0$ and to $-1$ asymptotically. The minimum is located at $r \approx 2.08$ a.u., i.e., at the equilibrium position of each H atom; its depth and sharpness depend on the orientation and whether the angular average has been performed or not.

The model potential (12) proposed in this work can certainly be improved in many respects, some of which are under current investigation. One of them is inclusion of exchange. Also, as we use an independent particle approximation, some many-body aspects (i.e., correlation) are only included indirectly through the use of MO in Eq. (12) but not explicitly.

### 5.2.2 Driven Equation and Cross Section

To introduce our Sturmian approach, we start with the use of an arbitrary potential $U(\mathbf{r})$, such as the one given by Eq. (12). We describe the PI process using first-order perturbation theory for a molecule that interacts with a radiation field. The Hamiltonian can be written as

$$\widehat{\mathcal{H}} = \widehat{H}_0 + \widehat{W}(t), \tag{16}$$

where $\widehat{H}_0 = \widehat{T} + U\left(\mathbf{r},\hat{\mathfrak{R}}\right)$ is the field-free Hamiltonian of the target with $\hat{\mathfrak{R}} = (\alpha,\beta,\gamma)$ the set of Euler angles that specify the spatial orientation of the molecule; $\widehat{T}$ is the kinetic energy operator, and

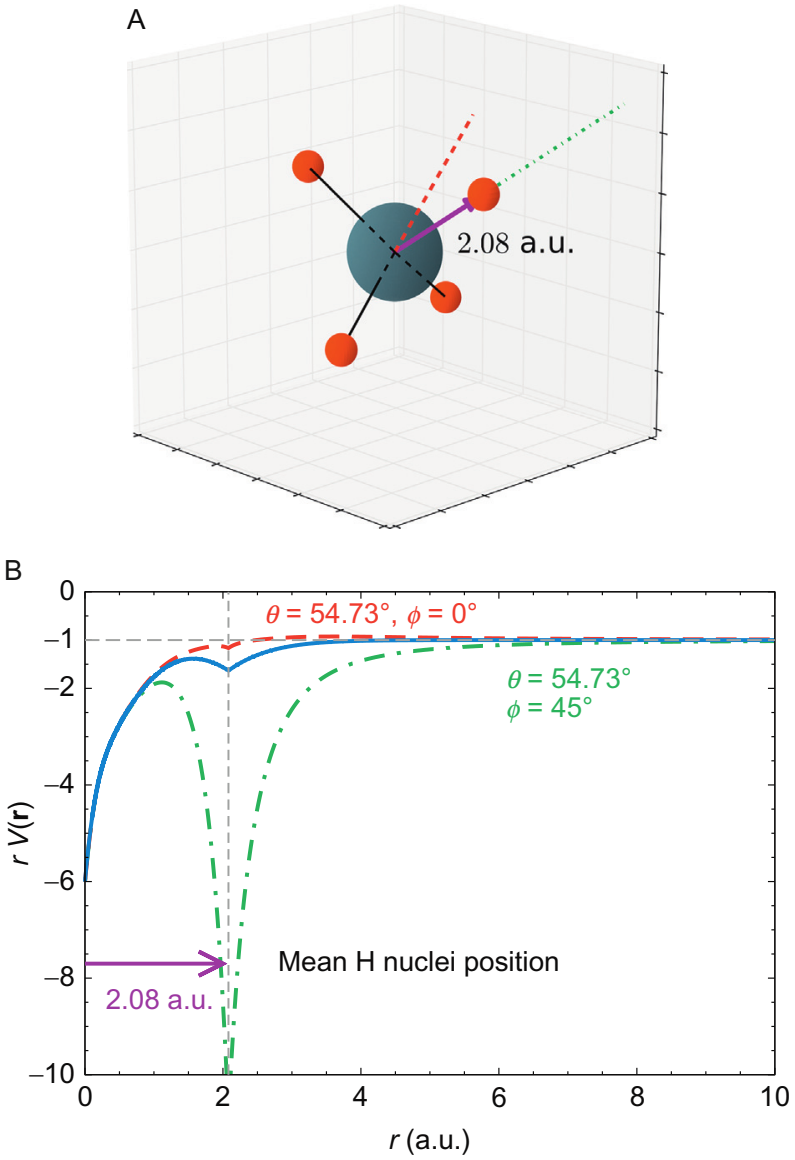


**Figure 6** *Upper panel*: Representation of the spatial localization of the individual atoms on $CH_4$; the mean equilibrium distance is indicated. *Bottom panel*: Molecular model (12) (red (dark gray in the print version) dash and green (gray in the print version) dash-dot) and angular averaged (15) (blue (dark gray in the print version), solid) potentials for $CH_4$, at indicated angles. The potential in green (gray in the print version) (dash-dot) corresponds to the variation of the potential on the green (gray in the print version) (dot) path on the figure of the upper panel.

$$\widehat{W}(t) = \begin{cases} -F^{(\mathrm{L})}(t) & \hat{\varepsilon}\cdot\mathbf{r} = F(t)\widehat{D}^{(\mathrm{L})}, \quad \text{length gauge} \\ -F^{(\mathrm{V})}(t) & \hat{\varepsilon}\cdot\mathbf{p} = F(t)\widehat{D}^{(\mathrm{V})}, \quad \text{velocity gauge} \end{cases} \tag{17}$$

where $F^{(\mathrm{g})}(t)$ is the electric field in the length gauge or the vector potential in the velocity gauge, $\hat{\boldsymbol{\varepsilon}}$ gives the polarization of the field and $\widehat{D}$ are the dipolar operators (2); $F(t)$ contains the time-dependent profile of the radiation field.

Dropping the explicit $\hat{\mathfrak{R}}$-dependence for the moment, we begin with the TDSE for the total Hamiltonian (16)

$$\left(i\frac{\partial}{\partial t}-\widehat{\mathcal{H}}\right)\Psi(\mathbf{r},t)=\left(i\frac{\partial}{\partial t}-\widehat{H}_0-\widehat{W}(t)\right)\Psi(\mathbf{r},t)=0, \tag{18}$$

and propose the general solution to be

$$\Psi(\mathbf{r},t)=\mathrm{e}^{-i\omega_0 t}\left[\Phi^{(0)}(\mathbf{r})+\Psi_{\mathrm{scatt}}(\mathbf{r},t)\right], \tag{19}$$

where $\Phi^{(0)}(\mathbf{r})$ is the wavefunction of the initial ground state of the molecule, usually the active MO to ionize, with energy $E_0=\omega_0$, and $\Psi_{\mathrm{scatt}}(\mathbf{r},t)$ is the wavefunction of the photoelectron, with energy $\omega=E$ (in atomic units). Replacing (19) in (18), we obtain

$$\left[i\frac{\partial}{\partial t}-\omega_0-\widehat{H}_0-\widehat{W}(t)\right]\Psi_{\mathrm{scatt}}(\mathbf{r},t)=\widehat{W}(t)\Phi^{(0)}(\mathbf{r}). \tag{20}$$

Now, if we apply a Fourier transform to (20), we obtain the TISE

$$\begin{aligned}\left(\omega-\omega_0-\widehat{H}_0\right)\Psi_{\mathrm{scatt}}(\mathbf{r},\omega)-\frac{1}{\sqrt{2\pi}}\int_{-\infty}^{\infty}\mathrm{d}\omega'\,\widehat{\mathcal{W}}(\omega')\Psi_{\mathrm{scatt}}(\mathbf{r},\omega-\omega')\\=\widehat{\mathcal{W}}(\omega)\Phi^{(0)}(\mathbf{r}),\end{aligned} \tag{21}$$

where $\widehat{\mathcal{W}}(\omega)$ is the Fourier transform of $\widehat{W}(t)$.

Equation (21) contains the interaction with the field to all orders, and therefore $\Psi_{\mathrm{scatt}}(\mathbf{r},\omega)$ contains information over all possible processes. Neglecting the integral term of (21), we can introduce a perturbation expansion on the scattering wavefunction.[26] Since we are interested here only in single PI processes, we retain the first order, and then Eq. (21) results in the driven equation for the final state wavefunction

$$\left(\omega-\omega_0-\widehat{H}_0\right)\Psi^{(1)}(\mathbf{r},\omega)=\widehat{\mathcal{W}}(\omega)\Phi^{(0)}(\mathbf{r}). \tag{22}$$

This is the equation that we want to solve; the scattering wavefunction at first order, $\Psi^{(1)}(\mathbf{r},\omega)$, will provide the PI information.

To solve Eq. (22), we separate first the scattering wavefunction in its radial and angular parts

$$\Psi^{(1)}(\mathbf{r},\omega)=\frac{1}{r}\sum_{\ell m}\varphi_\ell(r,\omega)\,Y_\ell^m(\hat{r}). \tag{23}$$

Usually, the radial wavefunction $\varphi_\ell(r,\omega)$ is expanded in some radial basis set. Within our Sturmian approach it is expanded in a GSF set (see Section 5.1)

$$\varphi_\ell(r,\omega) = \sum_j a_j^{(\ell,\,E)}(\omega)\mathcal{S}_j^{(\ell,\,E)}(r). \tag{24}$$

Performing an angular projection, Eq. (22) is converted into a set of angular-coupled differential equations

$$\sum_{\ell m}\left[\left(\omega-\omega_0+\frac{1}{2}\frac{\mathrm{d}^2}{\mathrm{d}r^2}-\frac{\ell(\ell+1)}{2r^2}\right)\delta_{\ell'\ell}\delta_{m'm}-U_{\ell'\ell}^{m'm}(r)\right]\varphi_\ell(r,\omega)=\varrho_{\ell'}^{m'}(r,\omega), \tag{25}$$

where $U_{\ell'\ell}^{m'm}(r)=\langle\ell'm'|U(\mathbf{r})|\ell m\rangle$ and $\varrho_{\ell'}^{m'}(r,\omega)=r\left\langle\ell'm'\middle|\widehat{\mathcal{W}}(\omega)\middle|\Phi^{(0)}\right\rangle$. As mentioned in Section 1, the use of a noncentral potential to describe the molecular target couples directly the different angular momenta of the initial state. For atoms or angular averaged molecular potentials, on the other hand, there is no coupling, $U_{\ell'\ell}^{m'm}(r)$ is diagonal and we have a single radial equation

$$\left(\omega-\omega_0+\frac{1}{2}\frac{\mathrm{d}^2}{\mathrm{d}r^2}-\frac{\ell(\ell+1)}{2r^2}-U(r)\right)\varphi_\ell(r,\omega)=\varrho_\ell^m(r,\omega). \tag{26}$$

Recall now that the potential $U\left(\mathbf{r},\hat{\mathfrak{R}}\right)$ of the field-free Hamiltonian $\widehat{H}_0$ contains the orientation $\hat{\mathfrak{R}}$ of the molecule. This orientation dependence is to be accounted for by $\varphi_\ell(r,\omega)$ and finally by the coefficients $a_j^{(\ell,\,E)}(\omega)$, so that we actually have $a_j^{(\ell,\,E)}\left(\omega,\hat{\mathfrak{R}}\right)$.

Now, to solve the coupled system of Eq. (25), we use the GSF expansion (24) and obtain

$$\sum_{\ell m}\sum_j a_j^{(\ell,\,E)}\left(\omega,\hat{\mathfrak{R}}\right)\left[\left(\omega-\omega_0+\frac{1}{2}\frac{\mathrm{d}^2}{\mathrm{d}r^2}-\frac{\ell(\ell+1)}{2r^2}\right)\delta_{\ell'\ell}\delta_{m'm}-U_{\ell'\ell}^{m'm}(r)\right]\times\mathcal{S}_j^{(\ell,\,E)}(r)=\varrho_{\ell'}^{m'}(r,\omega). \tag{27}$$

The final step consists in projecting (27) on $\mathcal{S}_i^{(\ell,\,E)}(r)$ (note that it is not the complex conjugate, see Eq. (11)): then, all the resulting matrices are calculated as indicated in Refs. 22 and 23. Solving the matrix problem with standard numerical methods provides the coefficients $a_j^{(\ell,\,E)}\left(\omega,\hat{\mathfrak{R}}\right)$.

All GSFs of the basis set have the same and correct asymptotic behavior, in this case the behavior dictated by the Coulomb potential (see Section 5.1). This means that our basis functions possess, by construction, important physical information and need to expand essentially the inner region, whose size will be determined by the range of the driven term. This makes the basis set adequate and finally computationally efficient. From the asymptotic property of the GSFs, we obtain the transition amplitude directly from the expansion coefficients of the scattering wavefunction in (24)[270]

$$\mathcal{T}\left(\omega,\hat{r},\hat{\mathfrak{R}}\right)=-\sqrt{2\pi}\left\langle\Psi_{\mathbf{k}}^{(-)}\middle|\widehat{\mathcal{W}}(\omega)\middle|\Phi^{(0)}\right\rangle=\sum_{\ell mj}a_j^{(\ell,E)}\left(\omega,\hat{\mathfrak{R}}\right)\mathrm{e}^{-i\left(\delta_\ell-\ell\frac{\pi}{2}\right)}Y_\ell^m(\hat{r}). \tag{28}$$

After an angular projection, we finally have the PI cross section as a function of the photon energy[270]

$$\frac{\mathrm{d}\sigma^{(\ell)}\left(\hat{\mathfrak{R}}\right)}{\mathrm{d}E}=\frac{4\pi^2\,\omega_{ki}^{(\mathrm{g})}}{c}\,k\,\frac{1}{2\pi}\frac{\left|\sum_j a_j^{(\ell,\,E)}\left(\omega,\hat{\mathfrak{R}}\right)\right|^2}{\left|\mathscr{F}(\omega)\right|^2}. \tag{29}$$

where $\omega^{(\mathrm{L})}=E-E_0$ or $\omega^{(\mathrm{V})}=(E-E_0)^{-1}$ is the difference between final and initial energies in either length or velocity gauges, and $\mathscr{F}(\omega)$ is the Fourier transform of the radiation field profile $F(t)$.

### 5.2.3 Example: Hydrogen Atom

The coupled system of Eq. (27) allows us to study PI processes for any potential. For systems that are described with a central potential, we are left with a single differential equation i.e. Eq. (26).[270–271] Applications to a set of different molecules will be given in Section 5.3 and is illustrated here for the hydrogen atom. For this atomic target, we solved the TISE (27) in both length and velocity gauges for electron energies in the range $[0.00, 3.00]$. Each one of these energies was used as the fixed energy $E$ to calculate our GSFs basis through Eq. (9), where a Coulomb potential with charge $-1$ was taken as auxiliary potential and a Yukawa potential with an energy-dependent parameter as generating potential. For the initial state, we used the exact ground state wavefunction of the atom. Our calculated PI cross section (29) is shown in Fig. 7, and is compared with the analytical formula given by Harriman.[272] Agreement between the cross sections in both gauges is perfect. Comparing with the analytical

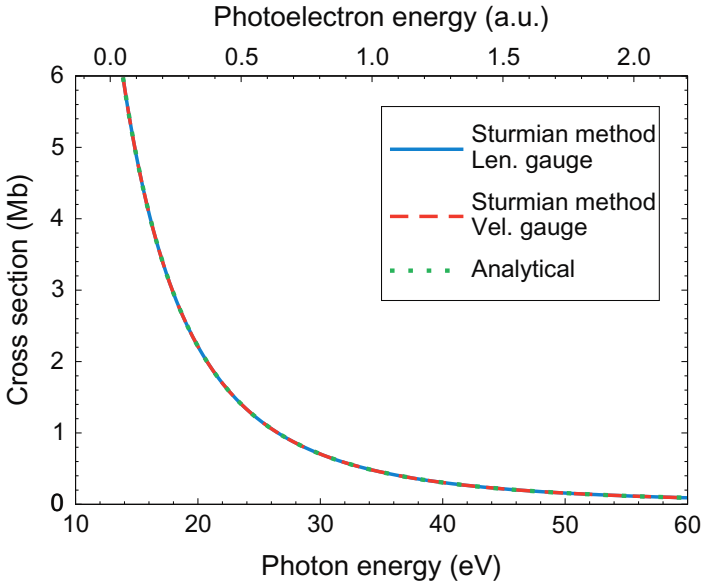


**Figure 7** PI cross section of H atom from the ground state 1*s*, in Mb versus photon energy in eV. Our results in length (blue (dark gray in the print version), solid) and velocity (red (dark gray in the print version), dash) gauges are compared with the exact analytical formula by Harriman[272] (green (gray in the print version), dots).

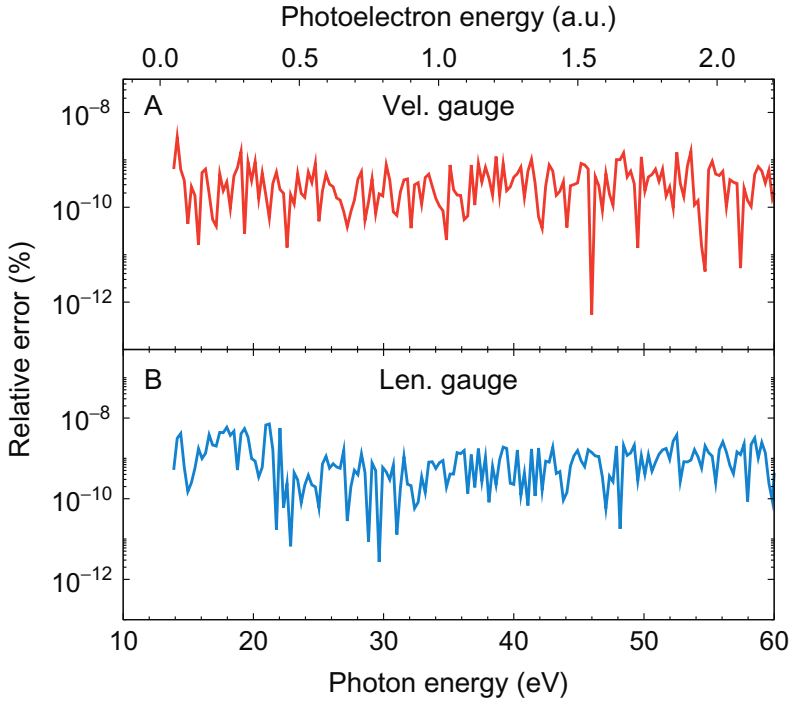


**Figure 8** Relative errors for the calculated PI cross sections presented in Fig. 7: (A) velocity gauge and (B) length gauge.

formula, we obtain errors of the order of $10^{-8} \sim 10^{-11}$ % over all the energy range (see Fig. 8), showing that our results with the selected GSF parameters gives very stable and "numerically exact" solutions to the TISE (22).

## 5.3 Results for Molecules

In this section, we report some results obtained by applying our Sturmian approach for molecular single PI, first solving Eq. (27) for the angular averaged potential (15), and then using the noncentral potential (12). Some results have been partially published before[271,273] for $CH_4$ and $H_2O$. The treatment of molecular systems with an averaged (central) potential is similar to that of atomic systems. For all cases, we used 60 GSFs for each final energy and final $(\ell, m)$ set; the basis functions are defined in a box of 50 a.u., using an auxiliary Coulomb potential with charge $-1$ and a generating Yukawa potential with an energy-dependent parameter. We have verified that in all cases the cross sections are converged in terms of number of GSFs. The initial MO were taken from Moccia's publications, specifically for $H_2O$ from Ref. 274, for $NH_3$ from Ref. 275 and for $CH_4$ from Ref. 276. For the calculation with the noncentral potential, with the fixed spatial molecular orientation given by Moccia, we use exactly the same GSF basis and initial MOs. The respective PI cross sections were calculated using Eq. (29), and we shall present our results in both length and velocity gauges. It is worth emphasizing here that the majority of theoretical publications on molecular PI present results obtained with the length gauge but do not provide a detailed analysis of gauge agreement, as often done for atomic systems.

### 5.3.1 $H_2O$

First, we start to study PI from the valence orbitals of $H_2O$ whose electronic ground state configuration is $1a_1^2\, 2a_1^2\, 1b_2^2\, 3a_1^2\, 1b_1^2\, {}^1A_1$. We study here only the two valence MOs. For the inner valence orbital $3a_1$ ($E_0 = -15.1323$ eV), the calculated PI cross sections are shown in Fig. 9, and for the outer orbital $1b_1$ ($E_0 = -13.4805$ eV) in Fig. 10. Both are compared with TD-DFT calculations by Stener et al.,[92] GIPM/D by Kilcoyne et al.,[156], STT by Cacelli et al.,[200] and ISM by Machado et al.[235]; the experimental data were reported by Banna et al.[277]

For the MO $3a_1$, we observe a good agreement between our results in velocity gauge and other theoretical calculations, in particular for photon energies beyond 30 eV, where our results are close to the TD-DFT and GIPM/D; on the other hand, the length gauge results considerably overestimate the cross sections for all calculated energies. In general, the cross sections for inner valence orbitals are difficult to calculate accurately, due to the presence of different many-body effects, such as relaxation of the core.

For the MO $1b_1$, the gauge discrepancy is of the same order as for the $3a_1$ case. Our cross sections compare fairly with other theoretical results, ours

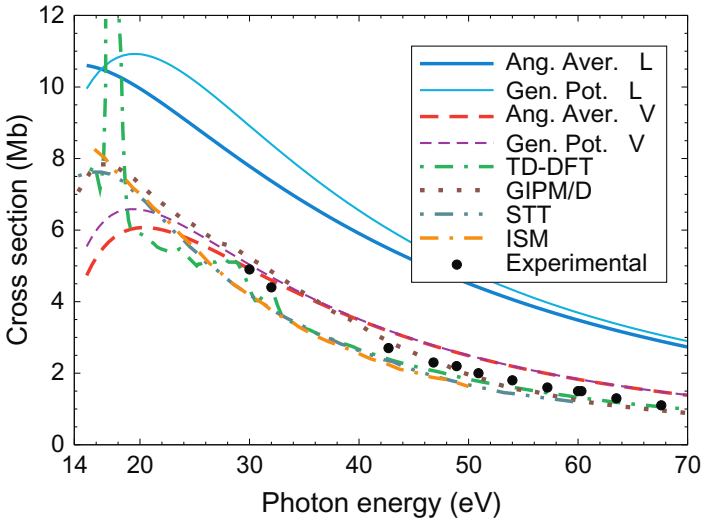


**Figure 9** Partial PI cross section in Mb versus photon energy in eV from the MO $3a_1$ of $H_2O$. Our results using the angular averaged molecular potential (15) for length (blue (dark gray in the print version), solid) and velocity (red (dark gray in the print version), dash) gauges, and using the noncentral potential (12) in length (light blue (gray in the print version), thin solid) and velocity (purple (dark gray in the print version), thin dash) gauges are compared with results for TD-DFT[92] (green (gray in the print version), dash-dot); GIPM/D[156] (brown (dark gray in the print version), dots); STT[200] (gray, dash-dot-dot); ISM[235] (orange (gray in the print version), dash-dash-dot) and with experimental data[277] (black dots).

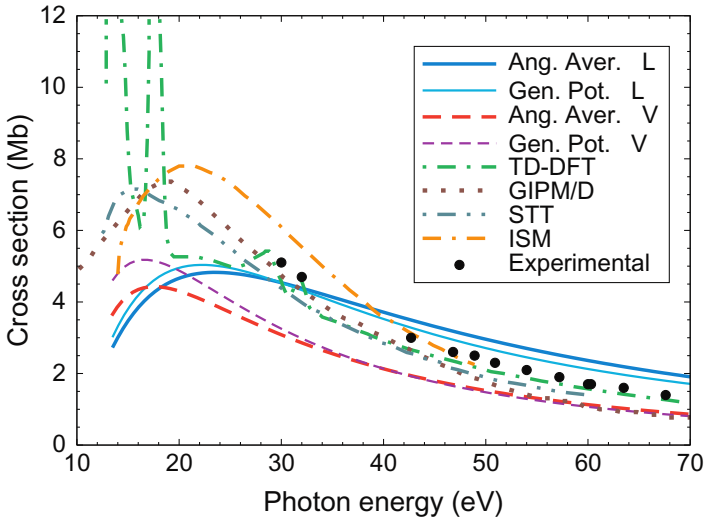


**Figure 10** Same as Fig. 9 for MO $1b_1$ of $H_2O$.

being seemingly too low in the threshold region where unfortunately no experimental data are available.

The results obtained using the noncentral potential (12), are only slightly better, indicating therefore that the central potential (15) is good enough to study this particular molecule.

### 5.3.2 $NH_3$

Next we study PI for both valence orbitals of $NH_3$ whose ground state electronic structure is $1a_1^2\,2a_1^2\,1e^4\,3a_1^2\,{}^1A_1$. For the inner valence MO $1e$ ($E_0 = -16.2071$ eV), the cross section is shown in Fig. 11, and for the outer valence MO $3a_1$ ($E_0 = -11.2819$ eV) in Fig. 12. Our results are compared

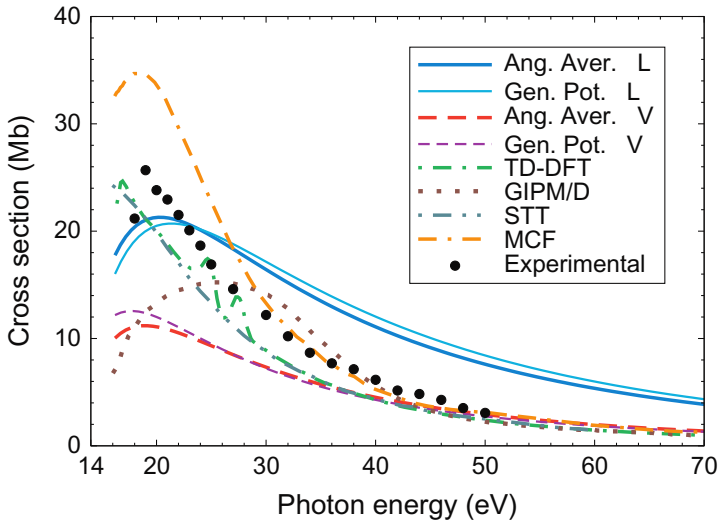


**Figure 11** Partial PI cross section in Mb versus photon energy in eV from the MO $1e$ of $NH_3$. Our results using the angular averaged potential (15) for length (blue (dark gray in the print version), solid) and velocity (red (dark gray in the print version), dash) gauges, and using the noncentral (12) in length (light blue (gray in the print version), thin solid) and velocity (purple (dark gray in the print version), thin dash) gauges, are compared with results for TD-DFT[92] (green (gray in the print version), dash-dot); GIPM/D[156] (brown (dark gray in the print version), dots); STT[200] (gray, dash-dot-dot); MCF[249] (orange (gray in the print version), dash-dash-dot) and with experimental data[278] (black dots).

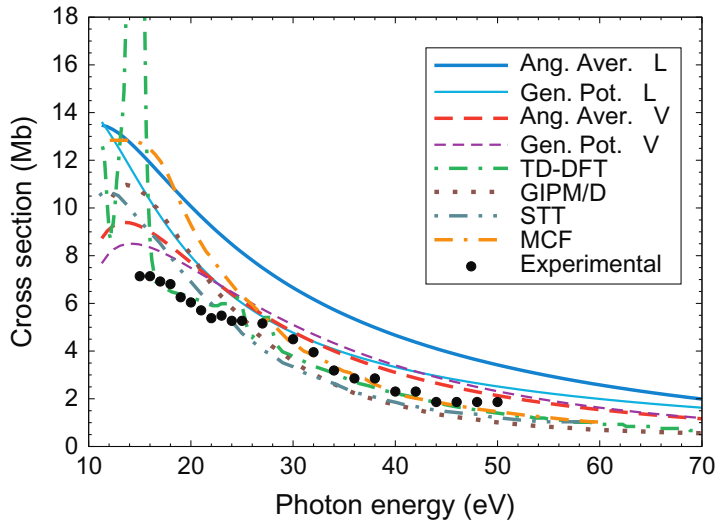


**Figure 12** Same as Fig. 11 for the MO $3a_1$ of $NH_3$.

with the TD-DFT results by Stener et al.,[92] GIPM/D by Kilcoyne et al.,[156] STT by Cacelli et al.,[200] and with calculations using MCF by Nascimento et al.[249]; the experimental data were reported by Brion et al.[278]

For the orbital $1e$, our results in velocity gauge show only a fair agreement with all reported data, in particular at high photon energies. Gauge discrepancy is again important and, fortuitously, the length gauge results reproduce the experimental magnitude around 22 eV.

For the orbital $3a_1$, our results show a slightly better gauge agreement; the length gauge cross section presenting the same shape but with a larger magnitude. The results in velocity gauge are in acceptable agreement with the experimental data over the whole energy range.

As for $H_2O$, the use of the noncentral potential (12) has a small effect, except in length gauge for the $3a_1$ orbital.

### 5.3.3 $CH_4$

Finally, we show our results for $CH_4$ whose ground state electronic structure is $1a_1^2\,2a_1^2\,1t_2^6\,{}^1A_1$. The calculated PI cross sections in both length and velocity gauges for the inner valence MO $2a_1$ ($E_0 = -25.0454$ eV) are shown in Fig. 13, and for the outer valence MO $1t_2$ ($E_0 = -13.7199$ eV) in Fig. 14. They are compared with TD-DFT calculations by Stener et al.,[92] GIPM/D by Kilcoyne et al.,[156] MS Xα by Rosi et al.,[133] and with STT by Cacelli et al.;[201] the experimental data are taken from Backx and van der Wiel.[279]

For the inner valence orbital $2a_1$, the length gauge calculation shows no agreement with any other calculations. For higher energies, say beyond 40 eV, we have a good agreement between our velocity results and experimental and other theoretical data.

For outer valence orbital $1t_2$, results obtained in velocity gauge show a fair agreement with experimental data, at least for photon energies higher than 30 eV; near threshold the position of the experimental peak is rather well reproduced but not its magnitude. Length gauge results are about a factor two too large.

For this molecule, the effect of using the noncentral potential (12) is almost unnoticeable for the $1t_2$ orbital but improves the velocity gauge result for the $2a_1$ orbital at lower energies.

As can be observed from Figs. 9 to 14, the Sturmian approach can give reasonable PI cross sections, in particular for ionization from the outer MOs. Some general features are: (i) little difference is seen between the use of the angular averaged (central) potential (15) and the noncentral potential (12)

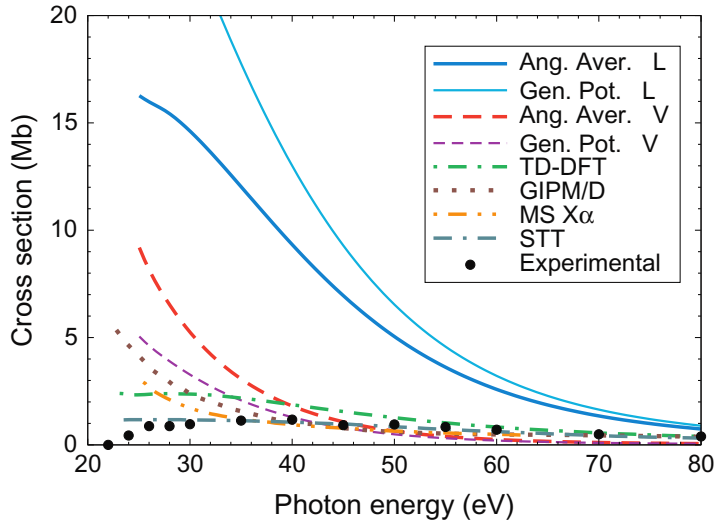


**Figure 13** Partial PI cross section in Mb versus photon energy in eV from the MO $2a_1$ of $CH_4$. Our results using the central potential (15) for length (blue (dark gray in the print version), solid) and velocity (red (dark gray in the print version), dash) gauges, and using the noncentral (12) for length (light blue (gray in the print version), thin solid) and velocity (purple (dark gray in the print version), thin dash) gauges, are compared with TD-DFT[92] (green (gray in the print version), dash-dot); GIPM/D[156] (brown (dark gray in the print version), dots); MSM[133] (orange (gray in the print version), dash-dot-dot); STT[201] (gray, dash-dash-dot) and with experimental data[279] (black dots).

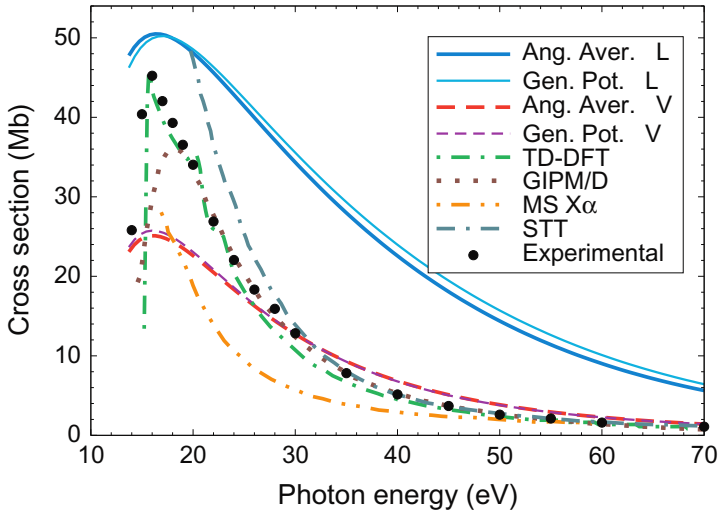


**Figure 14** Same as Fig. 13 for the MO $1t_2$ of $CH_4$.

(the latter improves marginally the cross sections); (ii) the length gauge results are systematically much larger over the whole energy range than those obtained with the velocity gauge, and are generally not in agreement with other data (experimental or theoretical). This discrepancy indicates that the initial state description needs to be improved; (iii) our velocity gauge results are in overall fair agreement with other theoretical cross sections, in particular for energies above, say, 15–20 eV over the ionization threshold;

(iv) exactly as illustrated in Section 3 with other molecules, the agreement between theoretical results (including ours) and experimental data is not uniform. For energies below 15 eV above ionization threshold agreement is generally poor.

## 6. CONCLUSIONS

In this contribution, we explored different theoretical aspects of PI of molecules. The description of this process requires solving quantum mechanically a very difficult many-body and multicenter problem. Contrary to molecular electronic structure calculations, one needs to evaluate a continuum state with appropriate asymptotic conditions. To make calculations feasible, a number of approximations must be made. Moreover, over the years, a range of theoretical methods and numerical techniques have been proposed. Among them, one finds those familiar in quantum chemistry such as HF, CI, and DFT, but also others, such as the RMM, CS or RPA, which encountered great success in atomic scattering calculations and were extended to molecular targets. Since in most experiments the molecules are randomly oriented, an average of the cross sections must be performed over all spatial orientations. This is an extra computational challenge that does not appear when studying collisions with atomic targets.

We began (Section 3) by describing the degree of theoretical–experimental agreement one may find in the literature. The PI of the valence orbitals of $H_2$, $N_2$, $CO_2$, and $C_6H_6$, are taken as an illustration and pinpoint some of the challenges one is confronted with. Except for $H_2$, a nonuniform picture arises. Agreement between theoretical results and experimental data is not always satisfactory; moreover, depending on the molecular orbital which is ionized and the energy range, severe discrepancies are often observed between different calculations. This is due to both the approximations made and the technique adopted. For this reason, we provided, in Section 4, a brief description of each method, together with the list of molecules to which they are applied.

We then introduced (Section 5) our Sturmian approach for PI. Essentially, the method provides one-electron basis functions (named Generalized Sturmian Functions) with appropriately chosen asymptotic boundary conditions. As they intrinsically contain this property, the basis functions are particularly adequate in describing the ionized electron continuum state. We briefly described how the Sturmian method, developed originally for atoms, may be implemented for molecules with a noncentral molecular potential.

As indicated above, in order to reduce the complexity of the problem, different approximations must be considered to make it tractable. In this very first implementation of the Sturmian approach, we started with the OCE and the SAE approximations. These reduce considerably the dimension of the problem and allow one to deal with one-electron wavefunctions, an ideal starting point to test the versatility of our method for molecules. It is well known that these approximations are good enough to study symmetric molecules, and in particular the ones with a heavy nucleus in its center of mass; this is the case for the selected molecules in this work ($H_2O$, $NH_3$, and $CH_4$) for which we reported results for PI from their valence orbitals. We stress here that the computational procedure to obtain such results with an angular averaged molecular model potential (15) is exactly the same as that used to study PI in a hydrogen atom. The same GSF basis and initial state wavefunctions are used for calculations with the noncentral potential (12). It turns out that the use of the latter only slightly improves the calculated cross sections. A systematic gauge comparison clearly showed that the length gauge largely overestimates the spectra at all energies. Considering some of the crude approximations, we may state that the implemented technique yields velocity gauge cross sections in reasonable agreement with experimental data, in particular at higher photoelectron energies. Although clearly perfectible (see below), these results are promising since they demonstrate that we have a working computational tool to study the electronic spectra of different molecules.

Let us add a short comment on computational efficiency. As illustrated by several bound-state calculations reported in our review[22] (and references therein), the GSF method is able to deliver results with high accuracy and low computational cost. For scattering calculations, although there is not a rigorous way to perform efficiency comparisons, some estimations were given in Ref. 280 with studies of three-body atomic breakup problems. Comparisons between the GSF and state-of-the-art methods showed that our methodology improves the numerical efficiency by at least an order of magnitude. Recently, in a study of DPI of He,[25] the GSF method reproduced very precisely ECS differential cross sections with a substantial gain (more than 50%) in memory storage of Hamiltonian matrix. In the present molecular applications, the tool is similar. The built in properties make the GSF set very adequate (and, to our mind, efficient) to deal with scattering problems, here PI.

The use of the angular averaged molecular model potential, which is equivalent to include the random orientation of the molecule before the scattering calculations, gave us good results for high energies; for lower

energies a better description of the target is clearly necessary. Besides the molecular potential itself, in that regime all the many-body effects are important, and the wavefunction for the initial state should include all active electrons. In that respect, we tried to include exchange terms in different manners. In our preliminary attempts, such terms did not remove the observed gauge discrepancies; we are currently investigating other ways to include in our model both exchange and correlations effects. Furthermore, the interactions with all nuclei becoming important, a many-center wavefunction should be employed; this may lead in a very expensive description of the system from the computational point of view, particularly for polyatomic molecules.

The use of a noncentral molecular potential (12) gave slightly better results in the low photon energy regime, since it is a more realistic description of the molecule. However, in this case the cross sections must be calculated for any Euler angles set. The final angular average over all possible spatial orientations of the molecule in the laboratory frame (defined by the polarization of the radiation field) is then computationally much more expensive.

In all investigated systems, in particular for inner valence orbitals, we saw that our length gauge results are always overestimating experimental data. The gauge discrepancies are known (see, for instance, Refs. 90, 200, 201, 203, 271 or 281) but are rarely discussed in the literature for molecular cases. They can be related to the quality of the wavefunctions for the initial state and also by the absence of different many-body effects. In order to obtain a better gauge agreement, one would need to use more sophisticated wave functions and avoid the FC and SAE approximations, since in some cases the relaxation effects are important, as shown, e.g., by TD-DFT results (see Sections 3 and 4.3.2 and Figs. 10 and 14).

As a summary, we have presented here some results of a first implementation of our Sturmian approach to study PI of molecules. Improvements of calculated cross sections may be obtained using more realistic molecular potentials and initial wavefunctions. Investigations in this direction are under way and will be presented elsewhere. GSFs offer also a promising tool to study other ionization processes in molecular systems such as the single ionization by electron impact, the so-called $(e,2e)$ process.

## ACKNOWLEDGMENTS

We acknowledge the CNRS (PICS project No. 06304) and CONICET (project No. Dl 158114) for funding our French-Argentinian collaboration, and CONICET (PIP 201301/607). G.G. also thanks the support by PGI (24/F059) of the Universidad Nacional del Sur.

## APPENDIX. LIST OF PHOTOIONIZATION CALCULATIONS FOR DIFFERENT MOLECULES

We list here, molecule by molecule, the references of all applications of theoretical methods mentioned in Section 4.

Homonuclear diatomic

1. $H_2^+$ [109,110,115,116,119,212,214,252–254,255]
2. $H_2$ [28,33,34,36,37,58,60,61,76,77,111–113,117,119,122,129,146–148,151,154,155,165,166,168,169,177–179,196,218,237,253]
3. $D_2$ [28,166]
4. $Li_2$ [69]
5. $C_2$ [1]
6. $N_2$ [39–43,52,68,90,102,118,122,129,130,132,146–150,152,154,155,171,172,175,176,180–182,186,194,218]
7. $O_2$ [66]
8. $F_2$ [205]
9. $Cl_2$ [85]

Heteronuclear diatomic

10. $HeH^{2+}$ [255]
11. $HeH^+$ [59,170]
12. LiH [184]
13. CH [195]
14. OH [238]
15. HF [78,83,92,149,154,189,201]
16. $CN^-$ [172]
17. CO [35,41,45,52,68,72,93,94,102,103,129,132,147,149–152,172,204,220]
18. NO [122,171]
19. HCl [55,83,202]

Polyatomic

20. $BH_3$ [83]
21. $H_2O$ [83,92,147,149–152,155,156,172,189,197–200,235,242,271]
22. $NH_3$ [83,92,150,156,172,189,200,221,249]
23. LiCN [63]
24. $AlH_3$ [83]
25. $H_2S$ [83,147,150,183,203,242]
26. $PH_3$ [83,90,150]
27. $SiH_4$ [83,135,236]

28. $CO_2$[42,45–47,54,70,122,132,172]
29. $NO_2$[42,45,71,172]
30. $NO_2^-$[172]
31. $O_3$[56]
32. $C_2N_2$[42,149]
33. CaHN[149]
34. $C_2O_2$[85]
35. COS[132]
36. $NF_3$[139]
37. $CS_2$[50,132]
38. $CF_4$[96,97,133,234]
39. $PF_3$[136,139]
40. $CF_3Cl$[138]
41. $SiF_4$[135]
42. $SF_6$[42,222,233]
43. $CCl_4$[234]
44. $SiCl_4$[134,135]
45. $TiCl_4$[42]

Organic molecules

46. $CH_3$[242]
47. $CH_4$[67,83,92,133,146–148,150–152,156,172,189,201,234,239,271,273]
48. $CH_3I$[137]
49. $H_2CO$[242]
50. $C_2H_2$[40,95,99,152,172,182,185,232,240]
51. $C_2H_4$[51,99,131,146,147,151,172]
52. $C_2H_6$[172]
53. $C_2(CN)_2$[149]
54. $C_3H_6O$ (methyl-oxirane)[87]
55. $C_3H_8$[172]
56. $(CH_3)_2S$[150]
57. $C_4H_6$[64]
58. $C_4H_4O$ (furan)[149]
59. $C_4H_5N$ (pyrrole)[149]
60. $C_4H_4N_2$ (pyrimidine)[98]
61. $C_4H_4N_2$ (pyrazine)[98]
62. $C_4H_4N_2O_2$ (uracil)[88]
63. $C_6H_6$ (benzene)[49,51,52,86,206]
64. $C_6F_6$[150]

**65.** $C_4F_4N_2$[149]
**66.** $Cr(CO)_6$[42,85]
**67.** $C_{10}H_8$ (naphthalene)[86]
**68.** $C_{14}H_{10}$ (anthracene)[86]
**69.** $C_{16}H_{10}$ (pyrene)[86]

Fullerenes
**70.** $C_{20}$[188]
**71.** $C_{60}^{+}$[187]
**72.** $C_{60}$[100,188,241]

## REFERENCES


1. Padial, N. T.; Collins, L. A.; Schneider, B. I. Photoionization of Ground-State Molecular Carbon $C_2$. *Astrophys. J.* **1985**, *298*, 369.
2. Liedahl, D. A.; Paerels, F. Photoionization-Driven X-Ray Line Emission in Cygnus X-3. *Astrophys. J.* **1996**, *468*, L33.
3. Bautista, M. A.; Romano, P.; Pradhan, A. K. Resonance-Averaged Photoionization Cross Sections for Astrophysical Models. *Astrophys. J. Suppl. Ser.* **1998**, *118*, 259.
4. Dopita, M. A.; Meatheringham, S. J. Photoionization Modeling of Magellanic Cloud Planetary Nebulae. I. *Astrophys. J.* **1991**, *367*, 115.
5. García-Segura, G.; Langer, N.; Rożyczka, M.; Franco, J. Shaping Bipolar and Elliptical Planetary Nebulae: Effects of Stellar Rotation, Photoionization Heating, and Magnetic Fields. *Astrophys. J.* **1999**, *517*, 767.
6. Monteiro, H.; Schwarz, H. E.; Gruenwald, R.; Heathcote, S. Three-Dimensional Photoionization Structure and Distances of Planetary Nebulae. I. NGC 6369. *Astrophys. J.* **2004**, *609*, 194.
7. Mallard, G.; Miller, J. H.; Smyth, K. C. Resonantly Enhanced Two-Photon Photoionization of NO in an Atmospheric Flame. *J. Chem. Phys.* **1982**, *76*, 3483.
8. Robb, D. B.; Blades, M. W. State-of-the-Art in Atmospheric Pressure Photoionization for LC/MS. *Anal. Chim. Acta* **2008**, *627*, 34.
9. Levine, J. S.; Javan, A. Observation of Laser Oscillation in a 1-atm $CO_2$-$N_2$-He Laser Pumped by an Electrically Heated Plasma Generated Via Photoionization. *Appl. Phys. Lett.* **1973**, *22*, 55.
10. Killian, T. C.; Kulin, S.; Bergeson, S. D.; Orozco, L. A.; Orzel, C.; Rolston, S. L. Creation of an Ultracold Neutral Plasma. *Phys. Rev. Lett.* **1999**, *83*, 4776.
11. Amusia, M. Y.; Baltenkov, A. S. Effect of Plasma Oscillations of $C_{60}$ Collectivized Electrons on Photoionization of Endohedral Noble-Gas Atoms. *Phys. Rev. A.* **2006**, *73*, 062723.
12. Hubbell, J. H. Review of Photon Interaction Cross Section Data in the Medical and Biological Context. *Phys. Med. Biol.* **1999**, *44*, R1.
13. Stepanek, J.; Blattmann, H.; Laissue, J. A.; Lyubimova, N.; Di Michiel, M.; Slatkin, D. N. Physics Study of Microbeam Radiation Therapy with PSI-Version of Monte Carlo Code GEANT as a New Computational Tool. *Med. Phys.* **2000**, *27*, 1664.
14. Horsley, J. A.; Stöhr, J.; Hitchcock, A. P.; Newbury, D. C.; Johnson, A. L.; Sette, F. Resonances in the K Shell Excitation Spectra of Benzene and Pyridine: Gas Phase, Solid, and Chemisorbed States. *J. Chem. Phys.* **1985**, *83*, 6099.
15. Piancastelli, M. N.; Lindle, D. W.; Ferrett, T. A.; Shirley, D. A. The Relationship Between Shape Resonances and Bond Lengths. *J. Chem. Phys.* **1987**, *86*, 2765.

16. Sheehy, J. A.; Gil, T. J.; Winstead, C. L.; Farren, R. E.; Langhoff, P. W. Correlation of Molecular Valence- and K-shell Photoionization Resonances with Bond Lengths. *J. Chem. Phys.* **1989**, *91*, 1796.
17. Cassuto, A.; Mane, M.; Jupille, J. Ethylene Monolayer and Multilayer on Pt(111) Below 52 K: Determination of Bond Lengths by Near-Edge X-ray Fine Structure. *Surf. Sci. Lett.* **1991**, *249*, 8.
18. Tonner, B. P.; Kao, C. M.; Plummer, E. W.; Caves, T. C.; Messmer, R. P.; Salaneck, W. R. Intermolecular Screening in Core-Level Photoemission from the Nitric-Oxide Dimer. *Phys. Rev. Lett.* **1983**, *51*, 1378.
19. Stöhr, J.; Outka, D. A.; Baberschke, K.; Arvanitis, D.; Horsley, J. A. Identification of CH Resonances in the K-shell Excitation Spectra of Gas-Phase, Chemisorbed, and Polymeric Hydrocarbons. *Phys. Rev. B* **1987**, *36*, 2976.
20. Solomon, J. L.; Madix, R. J.; Stöhr, J. $\pi$ Bonded Intermediates in Alcohol Oxidation: Orientations of Allyloxy and Propargyloxy on Ag(110) by Near Edge X-Ray Absorption Fine Structure. *J. Chem. Phys.* **1988**, *89*, 5316.
21. Liu, A. C.; Stöhr, J.; Friend, C. M.; Madix, R. J. A Critical Interpretation of the Near-Edge X-ray Absorption Fine Structure of Chemisorbed Benzene. *Surf. Sci.* **1990**, *235*, 107.
22. Gasaneo, G.; Ancarani, L. U.; Mitnik, D. M.; Randazzo, J. M.; Frapiccini, A. L.; Colavecchia, F. D. Three-Body Coulomb Problems with Generalized Sturmian Functions. *Adv. Quantum Chem.* **2013**, *67*, 153.
23. Mitnik, D. M.; Colavecchia, F. D.; Gasaneo, G.; Randazzo, J. M. Computational Methods for Generalized Sturmians basis. *Comp. Phys. Comm.* **2011**, *182*(5), 1145.
24. Ambrosio, M. J.; Colavecchia, F. D.; Gasaneo, G.; Mitnik, D. M.; Ancarani, L. U. Double Ionization of Helium by Fast Electrons with the Generalized Sturmian Functions Method. *J. Phys. B: At. Mol. Opt. Phys.* **2015**, *48*, 055204.
25. Randazzo, J. M.; Mitnik, D.; Gasaneo, G.; Ancarani, L. U.; Colavecchia, F. D. Double photoionization of helium: a generalized Sturmian approach. *Eur. J. Phys. D* **2015**, *69*, 189.
26. Messiah, A. *Quantum Mechanics*. North-Holland: Amsterdam, 1972.
27. Sanz-Vicario, J.; Bachau, H.; Martín, F. Time-Dependent Theoretical Description of Molecular Autoionization Produced by Femtosecond xuv Laser Pulses. *Phys. Rev. A* **2006**, *73*, 033410.
28. Sansone, G.; Kelkensberg, F.; Pérez-Torres, J. F.; Morales, F.; Kling, M. F.; Siu, W.; Ghafur, O.; Johnsson, P.; Swoboda, M.; Benedetti, E.; Ferrari, F.; Lépine, F.; Sanz-Vicario, J. L.; Zherebtsov, S.; Znakovskaya, I.; L'huillier, A.; Ivanov, M. Y.; Nisoli, M.; Martín, F.; Vrakking, M. J. J. Electron Localization Following Attosecond Molecular Photoionization. *Nature* **2010**, *465*, 763.
29. Fernández, J.; Martín, F. Electron and Ion Angular Distributions in Resonant Dissociative Photoionization of $H_2$ and $D_2$ Using Linearly Polarized Light. *New J. Phys.* **2009**, *11*, 043020.
30. Chandra, N. Photoelectron Spectroscopic Studies of Polyatomic Molecules: I. Theory. *J. Phys. B: At. Mol. Phys.* **1987**, *20*, 3405.
31. Edmonds, A. R. *Angular Momentum in Quantum Mechanics*; Princeton University Press: Princeton, NJ, 1957.
32. Chung, Y. M.; Lee, E. M.; Masuoka, T.; Samson, J. A. R. Dissociative Photoionization of $H_2$ from 18 to 124 eV. *J. Chem. Phys.* **1993**, *99*, 885.
33. Kelly, H. P. The Photoionization Cross Section for $H_2$ from Threshold to 30 eV. *Chem. Phys. Lett.* **1973**, *20*, 547.
34. Sanz-Vicario, J.; Palacios, A.; Cardona, J.; Bachau, H.; Martín, F. Ab Initio Time-Dependent Method to Study the Hydrogen Molecule Exposed to Intense Ultrashort Laser Pulses. *J. Electron Spectros. Relat. Phenom.* **2007**, *161*, 182.

35. Hilton, P. R.; Nordholm, S.; Hush, N. S. Ground-State Inversion Method Applied to Calculation of Molecular Photoionization Cross-Sections by Atomic Extrapolation: Interference Effects at Low Energies. *J. Electron Spectros. Relat. Phenom.* **1980**, *18*, 101.
36. Martín, P. H. S.; Rescigno, T. N.; McKoy, V.; Henneker, W. H. Photoionization Cross Sections for $H_2$ in the Random Phase Approximation with a Square-Integrable Basis. *Chem. Phys. Lett.* **1974**, *29*, 496.
37. Raşeev, G. Variational Calculation of the Logarithmic Derivative of the Wavefunction: The Electronic Autoionisation Region in Photoionisation of $H_2$. *J. Phys. B: At. Mol. Phys.* **1985**, *18*, 423.
38. Plummer, E. W.; Gustafsson, T.; Gudat, W.; Eastman, D. E. Partial Photoionization Cross Sections of $N_2$ and CO Using Synchrotron Radiation. *Phys. Rev. A* **1977**, *15*, 2339.
39. Stratmann, R. E.; Bandarage, G.; Lucchese, R. R. Electron-Correlation Effects in the Photoionization of $N_2$. *Phys. Rev. A* **1995**, *51*, 3756.
40. Levine, Z. H.; Soven, P. Time-Dependent Local-Density Theory of Dielectric Effects in Small Molecules. *Phys. Rev. A* **1984**, *29*, 625.
41. Davenport, J. Ultraviolet Photoionization Cross Sections for $N_2$ and CO. *Phys. Rev. Lett.* **1976**, *36*, 945.
42. Stener, M.; Decleva, P.; Lisini, A. Molecular Photoionization Cross Sections by the Local Density LCAO Stieltjes Imaging Approach. *J. Electron Spectrosc. Relat. Phenom.* **1995**, *74*, 29.
43. Lucchese, R.; Raseev, G.; McKoy, V. Studies of Differential and Total Photoionization Cross Sections of Molecular Nitrogen. *Phys. Rev. A* **1982**, *25*, 2572.
44. Brion, C.; Tan, K. Partial Oscillator Strengths for the Photoionization of $N_2O$ and $CO_2$ (20-60 eV). *Chem. Phys.* **1978**, *34*, 141.
45. Kilcoyne, D. A. L.; Nordholm, S.; Hush, N. S. An Analysis of Photoionisation Cross Sections for Carbon Monoxide and Dioxide and Nitrous Oxide by Diffraction Theory. *Chem. Phys.* **1986**, *107*, 225.
46. Lucchese, R.; McKoy, V. Studies of Differential and Total Photoionization Cross Sections of Carbon Dioxide. *Phys. Rev. A* **1982**, *26*, 1406.
47. Harvey, A. G.; Brambila, D. S.; Morales, F.; Smirnova, O. An R-Matrix Approach to Electron-Photon-Molecule Collisions: Photoelectron Angular Distributions from Aligned Molecules. *J. Phys. B: At. Mol. Opt. Phys.* **2014**, *47*, 215005.
48. Carlson, T. A.; Gerard, P.; Krause, M. O.; Grimm, F. A.; Pullen, B. P. Photoelectron Dynamics of the Valence Shells of Benzene as a Function of Photon Energy. *J. Chem. Phys.* **1987**, *86*, 6918.
49. Venuti, M.; Stener, M.; Decleva, P. Valence Photoionization of $C_6H_6$ by the B-Spline One-Centre Expansion Density Functional Method. *Chem. Phys.* **1998**, *234*, 95.
50. Stener, M.; Fronzoni, G.; Decleva, P. Time-Dependent Density-Functional Theory for Molecular Photoionization with Noniterative Algorithm and Multicenter B-Spline Basis Set: $CS_2$ and $C_6H_6$ Case Studies. *J. Chem. Phys.* **2005**, *122*, 234301.
51. Kilcoyne, D. A. L.; Nordholm, S.; Hush, N. S. Photoionisation of Ethylene and Benzene: A Theoretical Analysis of Multicentre Diffraction Effects. *Chem. Phys.* **1986**, *107*, 255.
52. Wilhelmy, I.; Ackermann, L.; Görling, A.; Roösch, N. Molecular Photoionization Cross Sections by the Lobatto Technique. I. Valence Photoionization. *J. Chem. Phys.* **1994**, *100*, 2808.
53. Langhoff, P. W. Aspects of Electronic Configuration Interaction in Molecular Photoionization. In: Hinze, J. Ed.; Electron-Atom and Electron-Molecule Collisions; Springer: New York, NY, 1983.
54. Daasch, W. R.; Davidson, E. R.; Hazi, A. U. Oxygen K Hole Photoionization Cross Section of $CO_2$. *J. Chem. Phys.* **1982**, *76*, 6031.

55. van Dishoeck, E. F.; van Hemert, M. C.; Dalgarno, A. Photodissociation Processes in the HCl Molecule. *J. Chem. Phys.* **1982**, *77*, 3693.
56. Decleva, P.; De Alti, G.; Lisini, A. Theoretical Study of the Valence Photoelectron Spectrum of Ozone: An Analysis of Correlation Effects and Configuration Interaction (CI) Model Spaces. *J. Chem. Phys.* **1988**, *89*, 367.
57. Bachau, H.; Cormier, E.; Decleva, P.; Hansen, J. E.; Martín, F. Applications of *B*-splines in Atomic and Molecular Physics. *Rep. Prog. Phys.* **2001**, *64*, 1815.
58. Apalategui, A.; Saenz, A. Multiphoton Ionization of the Hydrogen Molecule $H_2$. *J. Phys. B: At. Mol. Opt. Phys.* **2002**, *35*, 1909.
59. Vanne, Y. V.; Saenz, A. Numerical Treatment of Diatomic Two-Electron Molecules Using a B-Spline Based CI Method. *J. Phys. B: At. Mol. Opt. Phys.* **2004**, *37*, 4101.
60. Fojón, O. A.; Fernández, J.; Palacios, A.; Rivarola, R. D.; Martín, F. Interferences Effects in $H_2$ Photoionization at High Energies. *J. Phys. B: At. Mol. Opt. Phys.* **2004**, *37*, 3035.
61. Dowek, D.; Pérez-Torres, J. F.; Picard, Y. J.; Billaud, P.; Elkharrat, C.; Houver, J. C.; Sanz-Vicario, J. L.; Martín, F. Circular Dichroism in Photoionization of $H_2$. *Phys. Rev. Lett.* **2010**, *104*, 233003.
62. Klamroth, T. Laser-Driven Electron Transfer through Metal-Insulator-Metal Contacts: Time-Dependent Configuration Interaction Singles Calculations for a Jellium Model. *Phys. Rev. B* **2003**, *68*, 245421.
63. Klinkusch, S.; Saalfrank, P.; Klamroth, T. Laser-Induced Electron Dynamics Including Photoionization: A Heuristic Model within Time-Dependent Configuration Interaction Theory. *J. Chem. Phys.* **2009**, *131*, 114304.
64. Sonk, J. A.; Schlegel, H. B. TD-CI Simulation of the Electronic Optical Response of Molecules in Intense Fields II: Comparison of DFT Functionals and EOM-CCSD. *J. Phys. Chem. A* **2011**, *115*, 11832.
65. Nesbet, R. K. *Variational Methods in Electron-Atom Scattering Theory*; Plenum: New York, NY, 1979.
66. Stratmann, R. E.; Lucchese, R. R. A Graphical Unitary Group Approach to Study Multiplet Specific Multichannel Electron Correlation Effects in the Photoionization of $O_2$. *J. Chem. Phys.* **1995**, *102*, 8493.
67. Dalgarno, A. The Photo-Ionization Cross Section of Methane. *Proc. Phys. Soc. A* **1952**, *65*, 663.
68. Schirmer, J.; Cederbaum, L.; Domcke, W.; von Niessen, W. Strong Correlation Effects in Inner Valence Ionization of $N_2$ AND CO. *Chem. Phys.* **1977**, *26*, 149.
69. Larkins, F. P.; Richards, J. A. Photoionisation and Auger Electron Emission from the Lithium Molecule: Calculations Using Multicentre Numerical Continuum Functions. *Aust. J. Phys.* **1986**, *39*, 809.
70. Saito, N.; Fanis, A. D.; Kubozuka, K.; Machida, M.; Takahashi, M.; Yoshida, H.; Suzuki, I. H.; Cassimi, A.; Czasch, A.; Schmidt, L.; Dörner, R.; Wang, K.; Zimmermann, B.; McKoy, V.; Koyano, I.; Ueda, K. Carbon K-shell Photoelectron Angular Distribution from Fixed-In-Space CO2 Molecules. *J. Phys. B: At. Mol. Opt. Phys.* **2003**, *36*, L25.
71. Saito, N.; Toffoli, D.; Lucchese, R. R.; Nagoshi, M.; De Fanis, A.; Tamenori, Y.; Oura, M.; Yamaoka, H.; Kitajima, M.; Tanaka, H.; Hergenhahn, U.; Ueda, K. Symmetry- and Multiplet-Resolved N 1s Photoionization Cross Sections of the $NO_2$ Molecule. *Phys. Rev. A* **2004**, *70*, 062724.
72. Semenov, S. K.; Cherepkov, N. A.; Jahnke, T.; Dörner, R. Theoretical Study of Vibrationally Resolved Photoionization for the C K-Shell of the CO Molecule. *J. Phys. B: At. Mol. Opt. Phys.* **2004**, *37*, 1331.
73. Ågren, H.; Carravetta, V.; Vahtras, O.; Pettersson, L. G. M. Direct SCF Direct Static-Exchange Calculations of Electronic Spectra. *Theor. Chem. Acc.* **1997**, *97*, 14.

74. Nest, M.; Klamroth, T.; Saalfrank, P. The Multiconfiguration Time-Dependent Hartree-Fock Method for Quantum Chemical Calculations. *J. Chem. Phys.* **2005**, *122*, 124102.
75. Alon, O. E.; Streltsov, A. I.; Cederbaum, L. S. Many-Body Theory for Systems with Particle Conversion: Extending the Multiconfigurational Time-Dependent Hartree Method. *Phys. Rev. A* **2009**, *79*, 022503.
76. Kato, T.; Kono, H. Time-Dependent Multiconfiguration Theory for Ultrafast Electronic Dynamics of Molecules in an Intense Laser Field: A Description in Terms of Numerical Orbital Functions. *J. Chem. Phys.* **2008**, *128*, 184102.
77. Haxton, D. J.; Lawler, K. V.; McCurdy, C. W. Multiconfiguration Time-Dependent Hartree-Fock Treatment of Electronic and Nuclear Dynamics in Diatomic Molecules. *Phys. Rev. A* **2011**, *83*, 063416.
78. Haxton, D. J.; Lawler, K. V.; McCurdy, C. W. Single Photoionization of Be and HF Using the Multiconfiguration Time-Dependent Hartree-Fock Method. *Phys. Rev. A* **2012**, *86*, 013406.
79. Hohenberg, P.; Kohn, W. Inhomogeneous Electron Gas. *Phys. Rev.* **1964**, *136*, B864.
80. Kohn, W.; Sham, L. J. Self-Consistent Equations including Exchange and Correlation Effects. *Phys. Rev.* **1965**, *140*, A1133.
81. van Leeuwen, R.; Baerends, E. J. Exchange-Correlation Potential with Correct Asymptotic Behavior. *Phys. Rev. A* **1994**, *49*, 2421.
82. Görling, A. New KS Method for Molecules Based on an Exchange Charge Density Generating the Exact Local KS Exchange Potential. *Phys. Rev. Lett.* **1999**, *83*, 5459.
83. Stener, M.; Decleva, P. Photoionization of First and Second Row Hydrides by the B-Spline One-Centre Expansion Density Functional Method. *J. Electron Spectros. Relat. Phenom.* **1998**, *94*, 195.
84. Stener, M.; Decleva, P. Photoionization of $CH_4$, $SiH_4$, $BH_3$ and $AlH_3$ by the B-Spline One-Centre Expansion Density Functional Method. *J. Electron Spectros. Relat. Phenom.* **1999**, *104*, 135.
85. Toffoli, D.; Stener, M.; Fronzoni, G.; Decleva, P. Convergence of the Multicenter B-Spline DFT Approach for the Continuum. *Chem. Phys.* **2002**, *276*, 25.
86. Woon, D. E.; Park, J. Photoionization of Benzene and Small Polycyclic Aromatic Hydrocarbons in Ultravioletprocessed Astrophysical Ices: A Computational Study. *Astrophys. J.* **2004**, *607*, 342.
87. Stranges, S.; Turchini, S.; Alagia, M.; Alberti, G.; Contini, G.; Decleva, P.; Fronzoni, G.; Stener, M.; Zema, N.; Prosperi, T. Valence Photoionization Dynamics in Circular Dichroism of Chiral Free Molecules: The Methyl-Oxirane. *J. Chem. Phys.* **2005**, *122*, 244303.
88. Toffoli, D.; Decleva, P.; Gianturco, F. A.; Lucchese, R. R. Density Functional Theory for the Photoionization Dynamics of Uracil. *J. Chem. Phys.* **2007**, *127*, 234317.
89. Runge, E.; Gross, E. K. U. Density-Functional Theory for Time-Dependent Systems. *Phys. Rev. Lett.* **1984**, *52*, 997.
90. Stener, M.; Decleva, P. Time-Dependent Density Functional Calculations of Molecular Photoionization Cross Sections: $N_2$ and $PH_3$. *J. Chem. Phys.* **2000**, *112*, 10871.
91. Zangwill, A.; Soven, P. Density-Functional Approach to Local-Field Effects in Finite Systems: Photoabsorption in the Rare Gases. *Phys. Rev. A* **1980**, *21*, 1561.
92. Stener, M.; Fronzoni, G.; Toffoli, D.; Decleva, P. Time Dependent Density Functional Photoionization of $CH_4$, $NH_3$, $H_2O$ and HF. *Chem. Phys.* **2002**, *282*, 337.
93. Stener, M.; Decleva, P.; Cacelli, I.; Moccia, R.; Montuoro, R. Response Function Study of CO Photoionization: Ab Initio SCF and Density Functional Results. *Chem. Phys.* **2001**, *272*, 15.

94. Stener, M. Photoionization of Oriented Molecules: A Time Dependent Density Functional Approach. *Chem. Phys. Lett.* **2002**, *356*, 153.
95. Fronzoni, G.; Stener, M.; Decleva, P. Valence and Core Photoionization Dynamics of Acetylene by TD-DFT Continuum Approach. *Chem. Phys.* **2004**, *298*, 141.
96. Toffoli, D.; Stener, M.; Fronzoni, G.; Decleva, P. Photoionization Cross Section and Angular Distribution Calculations of Carbon Tetrafluoride. *J. Chem. Phys.* **2006**, *124*, 214313.
97. Patanen, M.; Kooser, K.; Argenti, L.; Ayuso, D.; Kimura, M.; Mondal, S.; Plésiat, E.; Palacios, A.; Sakai, K.; Travnikova, O.; Decleva, P.; Kukk, E.; Miron, C.; Ueda, K.; Martín, F. Vibrationally Resolved C 1s Photoionization Cross Section of $CF_4$. *J. Phys. B: At. Mol. Opt. Phys.* **2014**, *47*, 124032.
98. Holland, D. M. P.; Potts, A. W.; Karlsson, L.; Stener, M.; Decleva, P. A Study of the Valence Shell Photoionisation Dynamics of Pyrimidine and Pyrazine. *Chem. Phys.* **2011**, *390*, 25.
99. Russakoff, A.; Bubin, S.; Xie, X.; Erattupuzha, S.; Kitzler, M. Time-Dependent Density-Functional Study of the Alignment-Dependent Ionization of Acetylene and Ethylene by Strong Laser Pulses. *Phys. Rev. A* **2015**, *91*, 023422.
100. Madjet, M. E.; Chakraborty, H. S.; Rost, J. M.; Manson, S. T. Photoionization of $C_{60}$: A Model Study. *J. Phys. B: At. Mol. Opt. Phys.* **2008**, *41*, 105101.
101. Stener, M.; Toffoli, D.; Fronzoni, G.; Decleva, P. Recent Advances in Molecular Photoionization by Density Functional Theory Based Approaches. *Theor. Chem. Acc.* **2007**, *117*, 943.
102. Plésiat, E.; Decleva, P.; Martín, F. Vibrationally Resolved Photoelectron Angular Distributions from Randomly Oriented and Fixed-in-Space $N_2$ and CO Molecules. *J. Phys. B: At. Mol. Opt. Phys.* **2012**, *45*, 194008.
103. Kukk, E.; Ayuso, D.; Thomas, T. D.; Decleva, P.; Patanen, M.; Argenti, L.; Plésiat, E.; Palacios, A.; Kooser, K.; Travnikova, O.; Mondal, S.; Kimura, M.; Sakai, K.; Miron, C.; Martín, F.; Ueda, K. Effects of Molecular Potential and Geometry on Atomic Core-Level Photoemission over an Extended Energy Range: The Case Study of the CO Molecule. *Phys. Rev. A* **2013**, *88*, 033412.
104. Reinhardt, W. P. Complex Coordinates in the Theory of Atomic and Molecular Structure and Dynamics. *Ann. Rev. Phys. Chem.* **1982**, *33*, 223.
105. Moiseyev, N. Quantum theory of Resonances: Calculating Energies, Widths and Cross-Sections by Complex Scaling. *Phys. Rep.* **1998**, *302*, 212.
106. Nicolaides, C. A.; Beck, D. R. The Variational Calculation of Energies and Widths of Resonances. *Phys. Lett. A* **1978**, *65*, 11.
107. Simon, B. The Definition of Molecular Resonance Curves by the Method of Exterior Complex Scaling. *Phys. Lett. A* **1979**, *71*, 211.
108. McCurdy, C. W.; Martín, F. Implementation of Exterior Complex Scaling in B-Splines to Solve Atomic and Molecular Collision Problems. *J. Phys. B: At. Mol. Opt. Phys.* **2004**, *37*, 917.
109. McCurdy, C. W.; Rescigno, T. N. Complex-Basis-Function Calculations of Resolvent Matrix Elements: Molecular Photoionization. *Phys. Rev. A* **1980**, *21*, 1499.
110. Rescigno, T. N.; McCurdy, C. W. Locally Complex Distortions of the Energy Spectrum in the Calculation of Scattering Amplitudes and Photoionization Cross Sections. *Phys. Rev. A* **1985**, *31*, 624.
111. Vanroose, W.; Martín, F.; Rescigno, T. N.; McCurdy, C. W. Nonperturbative Theory of Double Photoionization of the Hydrogen Molecule. *Phys. Rev. A* **2004**, *70*.
112. Vanroose, W.; Horner, D. A.; Martín, F.; Rescigno, T. N.; McCurdy, C. W. Double Photoionization of Aligned Molecular Hydrogen. *Phys. Rev. A* **2006**, *74*, 052702.

113. Rescigno, T. N.; Vanroose, W.; Horner, D. A.; Martín, F.; McCurdy, C. W. First Principles Study of Double Photoionization of $H_2$ Using Exterior Complex Scaling. *J. Electron Spectros. Relat. Phenom.* **2007**, *161*, 85.
114. Light, J. C.; Hamilton, I. P.; Lill, J. V. Generalized Discrete Variable Approximation in Quantum Mechanics. *J. Chem. Phys.* **1985**, *82*, 1400.
115. Tao, L.; McCurdy, C. W.; Rescigno, T. N. Grid-Based Methods for Diatomic Quantum Scattering Problems: A Finite-Element Discrete-Variable Representation in Prolate Spheroidal Coordinates. *Phys. Rev. A* **2009**, *79*, 012719.
116. Tao, L.; McCurdy, C. W.; Rescigno, T. N. Grid-Based Methods for Diatomic Quantum Scattering Problems. II. Time-Dependent Treatment of Single- and Two-Photon Ionization of $H_2^+$. *Phys. Rev. A* **2009**, *80*, 013402.
117. Tao, L.; McCurdy, C. W.; Rescigno, T. N. Grid-Based Methods for Diatomic Quantum Scattering Problems. III. Double Photoionization of Molecular Hydrogen in Prolate Spheroidal Coordinates. *Phys. Rev. A* **2010**, *82*, 023423.
118. Yu, C.-h.; Pitzer, R. M.; McCurdy, C. W. Molecular Photoionization Cross Sections by the Complex-Basis- Function Method. *Phys. Rev. A* **1985**, *32*, 2134.
119. Morita, M.; Yabushita, S. Photoionization Cross Sections of $H_2^+$ and $H_2$ with Complex Gaussian-Type Basis Functions Optimized for the Frequency-Dependent Polarizabilities. *J. Comput. Chem.* **2008**, *29*, 2471.
120. Collins, L. A.; Schneider, B. I. Linear-Algebraic Approach to Electron-Molecule Collisions: General Formulation. *Phys. Rev. A* **1981**, *24*, 2387.
121. Collins, L. A.; Schneider, B. I. 2. The Linear Algebraic Method for Electron-Molecule Collisions. In: Huo, M. W., Gianturco, F. A., Eds.; Computational Methods for Electron-Molecule Collisions; Springer: New York, NY, 1995.
122. Collins, L.; Schneider, B. Molecular Photoionization in the Linear Algebraic Approach: $H_2$, $N_2$, NO, and $CO_2$. *Phys. Rev. A* **1984**, *29*, 1695.
123. Schneider, B. I.; Collins, L. A. Ab Initio Optical Potentials Applied to Low-Energy e-$H_2$ and e-$N_2$ Collisions in the Linear-Algebraic Approach. *Phys. Rev. A* **1983**, *27*, 2847.
124. Agassi, D.; Gal, A. Scattering from Non-Overlapping Potentials. I. General Formulation. *Ann. Phys. (N.Y.)* **1973**, *75*, 56.
125. Korringa, J. On the Calculation of the Energy of a Bloch Wave in a Metal. *Physica* **1947**, *13*, 392.
126. Dill, D.; Dehmer, J. L. Electron-Molecule Scattering and Molecular Photoionization Using the Multiple-Scattering Method. *J. Chem. Phys.* **1974**, *61*, 692.
127. Johnson, K. H. Scattered-Wave Theory of the Chemical Bond. In: Lödwin, P. O. Ed.; Advances in Quantum Chemistry; 7. Academic: New York, NY, 1973.
128. Slater, J. C.; Johnson, K. H. Self-Consistent-Field X$\alpha$ Cluster Method for Polyatomic Molecules and Solids. *Phys. Rev. B* **1972**, *5*, 844.
129. Davenport, J. W. Multiple Scattering Theory of Photoemission. *Int. J. Quantum Chem.* **1977**, *12*, 89.
130. Dehmer, J. L.; Dill, D. Molecular Effects on Inner-Shell Photoabsorption. K-Shell Spectrum of $N_2$. *J. Chem. Phys.* **1976**, *65*, 5327–5334.
131. Grimm, F. A. Calculations of the Partial Differential Photoionization Cross Sections for the Valence Bands of Ethylene. *Chem. Phys.* **1983**, *81*, 315.
132. Grimm, F. A.; Carlson, T. A.; Dress, W. B.; Agron, P.; Thomson, J. O.; Davenport, J. W. Use of the Multiple-Scattering Method for Calculating the Asymmetry Parameter in the Angle-Resolved Photoelectron Spectroscopy of $N_2$, CO, $CO_2$, COS, and $CS_2$. *J. Chem. Phys.* **1980**, *72*, 3041.
133. Rosi, M.; Sgamellotti, A.; Tarantelli, F.; Andreev, V. A.; Gofman, M.; Nefedov, V. Theoretical Investigation of the Energy Dependence of Photoionization Cross-Sections and Angular Distributions of Photoemission of $CH_4$ and $CF_4$. *J. Electron Spectros. Relat. Phenom.* **1986**, *41*, 439.

134. Tse, J. S.; Liu, Z. F.; Bozek, J. D.; Bancroft, G. M. Multiple-Scattering X$\alpha$ Study of the Silicon and Chlorine Core-Level Photoabsorption Spectra of $SiCl_4$. *Phys. Rev. A* **1989**, *39*, 1791.
135. Ishikawa, H.; Fujima, K.; Adachi, H.; Miyauchi, E.; Fujii, T. Calculation of Electronic Structure and Photoabsorption Spectra of Monosilane Molecules $SiH_4$, $SiF_4$, and $SiCl_4$. *J. Chem. Phys.* **1991**, *94*, 6740.
136. Powis, I. Continuum MS-X$\alpha$ Calculations for Core and Outer Valence Shell Photoionization of $PF_3$. *Chem. Phys. Lett.* **1993**, *215*, 269.
137. Powis, I. A Theoretical CMS-X$\alpha$ Treatment of $CH_3I$ Photoionization Dynamics: Outer Valence Shell and Iodine 4d Levels. *Chem. Phys.* **1995**, *201*, 189.
138. Powis, I. Oriented Molecule Photoelectron Angular Distributions in the Vicinity of a Photoionization Shape Resonance: Continuum Multiple Scattering- X$\alpha$ Calculations for Valence Ionization of $CF_3Cl$. *J. Chem. Phys.* **1997**, *106*, 5013.
139. Jürgensen, A.; Cavell, R. G. Valence Shell Photoionization Energies and Cross-Sections of $NF_3$ and $PF_3$. *J. Electron Spectros. Relat. Phenom.* **2003**, *128*, 245.
140. Ellison, F. O. Theoretical Equations for Photoionization Cross Sections of Polyatomic Molecules in Plane-Wave and Orthogonalized Plane-Wave Approximations. *J. Chem. Phys.* **1974**, *61*, 507.
141. Kaplan, I. G.; Markin, A. P. Calculation of Photoionization Cross Sections of Molecular Systems. I. Equations for Photoionization Cross Sections in AMO LCAO Approximation. *Opt. Spectrosc.* **1968**, *24*, 475.
142. Kaplan, I. G.; Markin, A. P. Calculation of Photionization Cross Sections of Molecular Systems. II. Ethylene, Butadiene and Benzene. *Opt. Spectrosc.* **1968**, *25*, 275.
143. Lohr, L. L.; Robin, M. B. Theoretical Study of Photoionization Cross Sections for $\pi$-Electron Systems. *J. Am. Chem. Soc.* **1970**, *92*, 7241.
144. Thiel, W.; Schweig, A. Photoionization Cross Sections in the Valence Electron Approximation. I. Linear Molecules. *Chem. Phys. Lett.* **1971**, *12*, 49.
145. Schweig, A.; Thiel, W. Photoionization Cross Sections: He I and He II Photoelectron Spectra of Saturated Three-Membered Rings. *Chem. Phys. Lett.* **1973**, *21*, 541.
146. Rabalais, J. W.; Debies, T. P.; Berkosky, J. L.; Huang, J. J.; Ellison, F. O. Calculated Photoionization Cross Sections and Relative Experimental Photoionization Intensities for a Selection of Small Molecules. *J. Chem. Phys.* **1974**, *61*, 516.
147. Dewar, M. J. S.; Komornicki, A.; Thiel, W.; Schweig, A. Calculation of Photoionization Cross Sections Using Ab-initio Wavefunctions and the Plane Wave Approximation. *Chem. Phys. Lett.* **1975**, *31*, 286.
148. Huang, J. T. J.; Ellison, F. O. Angular Asymmetry Parameters of Photoelectrons from $H_2$, $N_2$ and $CH_4$; an Extended Orthogonalized Plane-Wave Calculation. *Chem. Phys. Lett.* **1975**, *32*, 196.
149. Beerlage, M. J. M.; Feil, D. A Modified Plane Wave Model for Calculating UV Photo-Ionization Cross-Sections. *J. Electron Spectros. Relat. Phenom.* **1977**, *12*, 161.
150. Schweig, A.; Thiel, W. Photoionization Cross Sections: Interpretation of Band Intensities in He I and He II Photoelectron Spectra. *J. Electron Spectros. Relat. Phenom.* **1974**, *3*, 27.
151. Hilton, P. R.; Nordholm, S.; Hush, N. S. Molecular Photoionization Cross Sections Calculated by an Effective Plane Wave Method. *Chem. Phys.* **1976**, *15*, 345.
152. Deleuze, M.; Pickup, B. T.; Delhalle, J. Plane Wave and Orthogonalized Plane Wave Many-Body Green's Function Calculations of Photoionization Intensities. *Mol. Phys.* **1994**, *83*, 655.
153. Hilton, P. R.; Nordholm, S.; Hush, N. S. The Ground State Inversion Potential Method: Application to the Calculation of Photoionization Cross Sections. *J. Chem. Phys.* **1977**, *67*, 5213.
154. Kilcoyne, D. A. L.; McCarthy, C.; Nordholm, S.; Hush, N. S.; Hilton, P. R. An Atomic Diffraction Theory of Molecular Photoionization Cross Sections. *J. Electron Spectros. Relat. Phenom.* **1985**, *36*, 153–185.

155. Hilton, P. R.; Hordholm, S.; Hush, N. S. Photoionization Cross Section of Water by an Atomic Extrapolation Method. *Chem. Phys. Lett.* **1979**, *64*, 515.
156. Kilcoyne, D. A. L.; Nordholm, S.; Hush, N. S. Diffraction Analysis of the Photoionisation Cross Sections of Water, Ammonia and Methane. *Chem. Phys.* **1986**, *107*, 213.
157. In: *Atomic and Molecular Processes, an R-Matrix Approach*; Burke, P. G.; Berrington, K. A., Eds.; Institute of Physics Publishing: Bristol, 1993.
158. Bartschat, K. The R-matrix with Pseudo-States Method: Theory and Applications to Electron Scattering and Photoionization. *Comput. Phys. Commun.* **1998**, *114*, 168.
159. Schneider, B. I. 8. An *R*-Matrix Approach to Electron-Molecule Collisions. In: *Computational Methods for Electron-Molecule Collisions;* Huo, M. W., Gianturco, F. A., Eds.; Springer: New York, NY, 1995.
160. Noble, C. J. 14. *R*-Matrix for Intermediate Energy Scattering and Photoionization. In: *Computational Methods for Electron-Molecule Collisions;* Huo, M. W., Gianturco, F. A., Eds.; Springer: New York, NY, 1995.
161. Schneider, B. I.; LeDourneuf, M.; Burke, P. G. Theory of Vibrational Excitation and Dissociative Attachment: An R-matrix Approach. *J. Phys. B: At. Mol. Phys.* **1979**, *12*, L365.
162. Burke, P. G.; Seaton, M. J. The Vicinity of an R-Matrix Pole. *J. Phys. B: At. Mol. Phys.* **1984**, *17*, L683.
163. Seaton, M. J. Use of the R Matrix Method for Bound-State Calculations. I. General Theory. *J. Phys. B: At. Mol. Phys.* **1985**, *18*, 2111.
164. Seaton, M. J. Outer-Region Contributions to Radiative Transition Probabilities. *J. Phys. B: At. Mol. Phys.* **1986**, *19*, 2601.
165. Tennyson, J.; Noble, C.; Burke, P. Continuum States of the Hydrogen Molecule With the R-Matrix Method. *Int. J. Quantum Chem.* **1986**, *XXIX*, 1033.
166. Tennyson, J. Fully Vibrationally Resolved Photoionization of $H_2$ and $D_2$. *J. Phys. B: At. Mol. Phys.* **1987**, *20*, L375.
167. Joachain, C. J. R-matrix-Floquet Theory of Multiphoton Processes: Concepts, Results and Perspectives. *J. Mod. Opt.* **2007**, *54*, 1859.
168. Burke, P. G.; Colgan, J.; Glass, D. H.; Higgins, K. R-matrix-Floquet Theory of Molecular Multiphoton Processes. *J. Phys. B: At. Mol. Opt. Phys.* **2000**, *33*, 143.
169. Colgan, J.; Glass, D. H.; Higgins, K.; Burke, P. G. R-matrix Floquet Theory of Molecular Multiphoton Processes: II. Multiphoton Ionization of $H_2$. *J. Phys. B: At. Mol. Opt. Phys.* **2001**, *34*, 2089.
170. Saenz, A. Photoabsorption and Photoionization of $HeH^+$. *Phys. Rev. A* **2003**, *67*, 033409.
171. Tashiro, M. Application of the R-Matrix Method to Photoionization of Molecules. *J. Chem. Phys.* **2010**, *132*, 134306.
172. Amusia, M. Y.; Cherepkov, N. A. Many-Electron Correlations in the Scattering Processes. *Case Stud. At. Phys.* **1975**, *5*, 47.
173. Amusia, M. Y. Theory of Photoionization: VUV and Soft X-Ray Frequency Region. In: Becker, U., Shirley, D. A., Eds.; VUV and Soft X-Ray Photoionization; Plenum: New York, NY, 1996.
174. Rowe, D. Equations-of-Motion Method and the Extended Shell Model. *Rev. Mod. Phys.* **1968**, *40*, 153.
175. Yabushita, S.; McCurdy, C.; Rescigno, T. Complex-Basis-Function Treatment of Photoionization in the Random-Phase Approximation. *Phys. Rev. A* **1987**, *36*, 3146.
176. Semenov, S.; Cherepkov, N.; Fecher, G.; Schönhense, G. Generalization of the Atomic Random-Phase-Approximation Method for Diatomic Molecules: $N_2$ Photoionization Cross-Section Calculations. *Phys. Rev. A* **2000**, *61*, 032704.
177. Semenov, S. K.; Cherepkov, N. A. Photoionization of the $H_2$ Molecule in the Random Phase Approximation. *J. Phys. B: At. Mol. Opt. Phys.* **2003**, *36*, 1409.

178. Schirmer, J.; Mertins, F. A New Approach to the Random Phase Approximation. *J. Phys. B: At. Mol. Opt. Phys.* **1996**, *29*, 3559.
179. Semenov, S. K.; Cherepkov, N. A. Generalization of the Atomic RPA Method for Diatomic Molecules: $H_2$ Photoionization Cross-Section Calculation. *Chem. Phys. Lett.* **1998**, *291*, 375.
180. Lucchese, R.; Zurales, R. Comparison of the Random-Phase Approximation with the Multichannel Frozen-Core Hartree-Fock Approximation for the Photoionization of $N_2$. *Phys. Rev. A* **1991**, *44*, 291.
181. Semenov, S.; Cherepkov, N. Generalization of Atomic Random-Phase-Approximation Method for Diatomic Molecules. II. $N_2$ K-shell Photoionization. *Phys. Rev. A* **2002**, *66*, 022708.
182. Montuoro, R.; Moccia, R. Photoionization Cross Sections Calculation with Mixed $L^2$ Basis Set: STOs Plus B-Splines. Results for $N_2$ and $C_2H_2$ by KM-RPA Method. *Chem. Phys.* **2003**, *293*, 281.
183. Cacelli, I.; Carravetta, V.; Moccia, R. Differential Photoionization Cross Section Calculations for $H_2S$ Using the Random Phase Approximation with L2 Basis Functions. *Chem. Phys.* **1994**, *184*, 213.
184. Carmona-Novillo, E.; Moccia, R.; Spizzo, P. Photoionization Cross Section and Asymmetry Parameter of LiH: A Mixed GTO/STOCOS $L^2$ Basis Set Calculation. *Chem. Phys.* **1996**, *210*, 435.
185. Yasuike, T.; Yabushita, S. Valence Photoionization and Autoionizing States of Acetylene Studied by the Complex Basis Function Method in the Random Phase Approximation. *Chem. Phys. Lett.* **2000**, *316*, 257.
186. Cherepkov, N.; Semenov, S.; Hikosaka, Y.; Ito, K.; Motoki, S.; Yagishita, A. Manifestation of Many-Electron Correlations in Photoionization of the K Shell of $N_2$. *Phys. Rev. Lett.* **2000**, *84*, 250.
187. Polozkov, R. G.; Ivanov, V. K.; Solov'yov, A. V. Photoionization of the Fullerene Ion $C_{60}^+$. *J. Phys. B: At. Mol. Opt. Phys.* **2005**, *38*, 4341.
188. Ivanov, V. K.; Kashenock, G. Y.; Polozkov, R. G.; Solov'yov, A. V. Photoionization Cross Sections of the Fullerenes $C_{20}$ and $C_{60}$ Calculated in a Simple Spherical Model. *J. Phys. B: At. Mol. Opt. Phys.* **2001**, *34*, L669.
189. Cacelli, I.; Carravetta, V.; Moccia, R.; Rizzo, A. Photoionization and Photoabsorption Cross Section Calculations in Methane, Ammonia, Water, and Hydrogen Fluoride Molecules. *J. Phys. Chem.* **1988**, *92*, 979.
190. Langhoff, P. W. Stieltjes Imaging of Atomic and Molecular Photoabsorption Profiles. *Chem. Phys. Lett.* **1973**, *22*, 60.
191. Langhoff, P. W. Stieltjes-Tchebycheff Moment-Tehory Approach to Molecular Photoionization Studies. In: *Electron-Molecule and Photon-Molecule Collisions* Rescigno, T., McKoy, V., Schneider, B., Eds.; Plenum: New York, NY, 1979.
192. Shohat, J. A.; Tamarkin, J. D. The Problem of Moments. *Mathematical Surveys,* 1. American Mathematical Society: Providence, RI, 1943.
193. Corcoran, C. T.; Langhoff, P. W. Moment-Theory Approximations for Nonnegative Spectral Densities. *J. Math. Phys.* **1977**, *18*, 651.
194. Rescigno, T. N.; Bender, C. F.; McKoy, B. V.; Langhoff, P. W. Photoabsorption in Molecular Nitrogen: A Moment Analysis of Discrete-Basis-Set Calculations in the Static-Exchange Approximation. *J. Chem. Phys.* **1978**, *68*, 970.
195. Barsuhn, J.; Nesbet, R. K. The Photoionization and Photodissociation of CH in the Vicinity of the Ionization Threshold. *J. Chem. Phys.* **1978**, *68*, 2783.
196. ONeil, S. V.; Reinhardt, W. P. Photoionization of Molecular Hydrogen. *J. Chem. Phys.* **1978**, *69*, 2126.
197. Williams, G. R. J.; Langhoff, P. W. Photoabsorption in $H_2O$: Stieltjes-Tchebycheff Calculations in the Time-Dependent Hartree-Fock Approximation. *Chem. Phys. Lett.* **1979**, *60*, 201.

198. Delaney, J. J.; Saunders, V. R.; Hillier, I. H. Stieltjes-Tchebycheff Calculations in the Static-Exchange Approximation of Photoexcitation and Ionisation in Water. *J. Phys. B: At. Mol. Phys.* **1981**, *14*, 819.
199. Diercksen, G. H. F.; Kraemer, W. P.; Rescigno, T. N.; Bender, C. F.; Mckoy, B. V.; Langhoff, S. R.; Langhoff, P. W. Theoretical Studies of Photoexcitation and Ionization in $H_2O$. *J. Chem. Phys.* **1982**, *76*, 1043.
200. Cacelli, I.; Moccia, R.; Carravetta, V. Photoionisation Cross Section Calculations for $H_2O$ and $NH_3$ by One-Center Expansion and Sticltjies Technique. *Chem. Phys.* **1984**, *90*, 313.
201. Cacelli, I.; Carravetta, V.; Moccia, R. Transition Probability and Photoionisation Cross Section Calculations for $CH_4$ and HF by One-Centre Expansion and Stieltjes Technique. *J. Phys. B: At. Mol. Phys.* **1985**, *18*, 1375.
202. Cacelli, I.; Carravetta, V.; Moccia, R. Photoionization Cross Section Calculations of HCl by the Stieltjes Technique. *Mol. Phys.* **1986**, *59*, 385.
203. Cacelli, I.; Carravetta, V.; Moccia, R. $H_2S$ Photoabsorption and Photoionization Cross Sections by Stieltjes Imaging. *Chem. Phys.* **1988**, *120*, 51.
204. Görling, A.; Rösch, N. Molecular Photo Cross Sections with the LCGTO-X$\alpha$ Method Using Stieltjes Imaging. *J. Chem. Phys.* **1990**, *93*, 5563.
205. Orel, A. E.; Rescigno, T. N.; Mckoy, B. V.; Langhoff, P. W. Photoexcitation and Ionization in Molecular Fluorine: Stieltjes-Tchebycheff Calculations in the Static-Exchange Approximation. *J. Chem. Phys.* **1980**, *72*, 1265.
206. Gokhberg, K.; Vysotskiy, V.; Cederbaum, L. S.; Storchi, L.; Tarantelli, F.; Averbukh, V. Molecular Photoionization Cross Sections by Stieltjes-Chebyshev Moment Theory Applied to Lanczos Pseudospectra. *J. Chem. Phys.* **2009**, *130*, 064104.
207. Kohn, W. Variational Methods in Nuclear Collision Problems. *Phys. Rev.* **1948**, *74*, 1763.
208. Rescigno, T. N.; McCurdy, C. W.; Orel, A. E.; Lengsfield, B. H., III 1. The Complex Kohn Variational Method. In: Huo, M. W., Gianturco, F. A., Eds.; Computational Methods for Electron-Molecule Collisions; Springer: New York, NY, 1995.
209. McCurdy, C. W.; Rescigno, T. N. Collisions of Electrons with Polyatomic Molecules: Electron-Methane Scattering by the Complex Kohn Variational Method. *Phys. Rev. A* **1989**, *39*, 4487.
210. Manolopoulos, D.; Wyatt, R. Quantum Scattering Via the Log Derivative Version of the Kohn Variational Principle. *Chem. Phys. Lett.* **1988**, *152*, 23.
211. Manolopoulos, D. E.; Wyatt, R. E.; Clary, D. C. Iterative Solution in Quantum Scattering Theory. The Log Derivative Kohn Approach. *J. Chem. Soc. Faraday Trans.* **1990**, *86*, 1641.
212. Le Rouzo, H.; Raşeev, G. Finite-Volume Variational Method: First Application to Direct Molecular Photoionization. *Phys. Rev. A* **1984**, *29*, 1214.
213. Manolopoulos, D. E. Lobatto Shape Functions. In: Cerjan, C. Ed.; Numerical Grid Methods and Their Application to Schrödinger's Equation; Springer: The Netherlands, 1993.
214. Rösch, N.; Wilhelmy, I. Representation of Electronic Wavefunctions by Lobatto Shape Functions: Application to the Photoionization Cross Section of $H_2^+$. *Chem. Phys. Lett.* **1992**, *189*, 499.
215. Wilhelmy, I.; Rösch, N. Molecular Photoionization Cross Sections by the Lobatto Technique. II. Core Level Photionization. *Chem. Phys.* **1994**, *185*, 317–332.
216. Orel, A. E.; Rescigno, T. N. Variational Expressions for First-Order Properties involving Continuum Wave Functions. *Phys. Rev. A* **1990**, *41*, 1695.
217. Rescigno, T.; Lengsfield, B.; McCurdy, C. Electronic Excitation of Formaldehyde by Low-Energy Electrons: A Theoretical Study Using the Complex Kohn variational Method. *Phys. Rev. A* **1990**, *41*, 2462.
218. Lynch, D. L.; Schneider, B. I. Molecular Photoionization Using the Complex Kohn Variational Method. *Phys. Rev. A* **1992**, *45*, 4494.

219. Nesbet, R. K. Comparison of the R-matrix and Hulthén-Kohn methods for a model multichannel scattering problem. *Phys. Rev. A* **1981**, *24*, 2975.
220. Rescigno, T. N.; Lengsfield, B. H.; Orel, A. E. Interchannel Coupling and Ground State Correlation Effects in the Photoionization of CO. *J. Chem. Phys.* **1993**, *99*, 5097.
221. Orel, A. E.; Rescigno, T. N. Photoionization of Ammonia. *Chem. Phys. Lett.* **1997**, *269*, 222.
222. Jose, J.; Lucchese, R. R.; Rescigno, T. N. Interchannel Coupling Effects in the Valence Photoionization of $SF_6$. *J. Chem. Phys.* **2014**, *140*, 204305.
223. Schwinger, J. Minutes of the Meeting at Stanford University, California July 11-12, 1947 [14]. *Phys. Rev.* **1947**, *72*, 738, See p. 742.
224. Lippmann, B. A.; Schwinger, J. Variational Principles for Scattering Processes. I. *Phys. Rev.* **1950**, *79*, 469.
225. Huo, W. M. 15. The Schwinger Variational Method. In: Huo, M. W., Gianturco, F. A., Eds.; Computational Methods for Electron-Molecule Collisions; Springer: New York, NY, 1995.
226. Taylor, J. R. *Scattering Theory: The Quantum Theory of Nonrelativistic Collisions*. Wiley: New York, 1972.
227. Lucchese, R. R.; McKoy, V. Application of the Schwinger variational principle to electron scattering. *J. Phys. B: At. Mol. Phys.* **1979**, *12*, L421.
228. Takatsuka, K.; McKoy, V. Extension of the Schwinger variational principle beyond the Static-Exchange Approximation. *Phys. Rev. A* **1981**, *24*, 2473.
229. Watson, D. K.; McKoy, V. Discrete-Basis-Function Approach to Electron-Molecule Scattering. *Phys. Rev. A* **1979**, *20*, 1474.
230. Lucchese, R. R.; Watson, D. K.; McKoy, V. Iterative Approach to the Schwinger Variational Principle for Electron-Molecule Collisions. *Phys. Rev. A* **1980**, *22*, 421.
231. Lucchese, R.; McKoy, V. Iterative Approach to the Schwinger Variational Principle Applied to ElectronMolecular-Ion Collisions. *Phys. Rev. A* **1981**, *24*, 770.
232. Lynch, D.; Lee, M. T.; Lucchese, R. R.; McKoy, V. Studies of the Photoionization Cross Sections of Acetylene. *J. Chem. Phys.* **1984**, *80*, 1907.
233. Natalense, A. P. P.; Lucchese, R. R. Cross Section and Asymmetry Parameter Calculation for Sulfur 1s Photoionization of $SF_6$. *J. Chem. Phys.* **1999**, *111*, 5344.
234. Natalense, A.; Brescansin, L.; Lucchese, R. Cross Section and Asymmetry Parameter Calculations for the C 1s Photoionization of $CH_4$, $CF_4$, and $CCl_4$. *Phys. Rev. A* **2003**, *68*, 032701.
235. Machado, L. E.; Brescansin, L. M.; Lima, M. A. P.; Braunstein, M.; McKoy, V. Cross Sections and Photoelectron Asymmetry Parameters for Photoionization of $H_2O$. *J. Chem. Phys.* **1990**, *92*, 2362.
236. Machado, L. E.; Lee, M. T.; Brescansin, L. M. Photoionization Cross Sections and Asymmetry Parameters for Silane. *J. Chem. Phys.* **1999**, *110*, 7228.
237. Machado, A. M.; Masili, M. Variationally Stable Calculations for Molecular Systems: Polarizabilities and Two-Photon Ionization Cross Section for the Hydrogen Molecule. *J. Chem. Phys.* **2004**, *120*, 7505.
238. Stephens, J. A.; McKoy, V. Photoionization of the Valence Orbitals of OH. *J. Chem. Phys.* **1988**, *88*, 1737.
239. Braunstein, M.; McKoy, V.; Machado, L. E.; Brescansin, L. M.; Lima, M. A. P. Studies of the Photoionization Cross Sections of $CH_4$. *J. Chem. Phys.* **1988**, *89*, 2998.
240. Wells, M.; Lucchese, R. R. The Inner Valence Photoionization of Acetylene. *J. Chem. Phys.* **1999**, *110*, 6365.
241. Gianturco, F.; Lucchese, R. Cross Sections and Asymmetry Parameters in Gas-Phase Photoionization of $C_60$. *Phys. Rev. A* **2001**, *64*, 032706.
242. Wiedmann, R. T.; White, M. G.; Wang, K.; McKoy, V. Rotationally Resolved Photoionization of Polyatomic Hydrides: $CH_3$, $H_2O$, $H_2S$, $H_2CO$. *J. Chem. Phys.* **1994**, *100*, 4738.

243. Horáček, J.; Sasakawa, T. Method of Continued Fractions with Application to Atomic Physics. *Phys. Rev. A* **1983**, *28*, 2151.
244. Horáček, J.; Sasakawa, T. Method of Continued Fractions with Application to Atomic Physics. II. *Phys. Rev. A* **1984**, *30*, 2274.
245. Lee, M. T.; Iga, I.; Fujimoto, M. M.; Lara, O. The Method of Continued Fractions for Electron (Positron)-Atom Scattering. *J. Phys. B: At. Mol. Opt. Phys.* **1995**, *28*, L299.
246. Lee, M. T.; Iga, I.; Fujimoto, M. M.; Lara, O. Application of the Method of Continued Fractions for Electron Scattering by Linear Molecules. *J. Phys. B: At. Mol. Opt. Phys.* **1995**, *28*, 3325.
247. Ribeiro, E. M. S.; Machado, L. E.; Lee, M. T.; Brescansin, L. M. Application of the Method of Continued Fractions to Electron Scattering by Polyatomic Molecules. *Comput. Phys. Commun.* **2001**, *136*, 117.
248. Machado, A.; Fujimoto, M.; Taveira, A.; Brescansin, L.; Lee, M. T. Application of the Method of Continued Fractions to Multichannel Studies on Electronic Excitation of $H_2$ by Electron Impact. *Phys. Rev. A* **2001**, *63*, 032707.
249. Nascimento, E. M.; Ribeiro, E. M. S.; Brescansin, L. M.; Lee, M. T.; Machado, L. E. Extension of the Method of Continued Fractions to Molecular Photoionization: An Application to Ammonia. *J. Phys. B: At. Mol. Opt. Phys.* **2003**, *36*, 3621.
250. Crank, J.; Nicolson, P. A practical Method for Numerical Evaluation of Solutions of Partial Differential Equations of the Heat-Conduction Type. *Proc. Cambridge Philos. Soc.* **1947**, *43*, 50.
251. Goldberg, A.; Shore, B. W. Modelling Laser Ionisation. *J. Phys. B: At. Mol. Phys.* **1978**, *11*, 3339.
252. Picón, A.; Bahabad, A.; Kapteyn, H. C.; Murnane, M. M.; Becker, A. Two-Center Interferences in Photoionization of a Dissociating $H_2^+$ Molecule. *Phys. Rev. A* **2011**, *83*, 013414.
253. Yuan, K. J.; Lu, H.; Bandrauk, A. Linear- and Circular-Polarization Photoionization Angular Distributions in $H_2$ and $H_2^+$ by Attosecond Xuv Laser Pulses. *Phys. Rev. A* **2011**, *83*, 043418.
254. Silva, R. E. F.; Catoire, F.; Rivière, P.; Bachau, H.; Martín, F. Correlated Electron and Nuclear Dynamics in Strong Field Photoionization of $H_2^+$. *Phys. Rev. Lett.* **2013**, *110*, 113001.
255. Bian, X. B. Photoionization of Atoms and Molecules Studied by the Crank-Nicolson Method. *Phys. Rev. A* **2014**, *90*, 033403.
256. Shull, H.; Loöwdin, P. O. Superposition of Configurations and Natural Spin Orbitals. Applications to the He Problem. *J. Chem. Phys.* **1959**, *30*, 617.
257. Goscinski, O. Conjugate Eigenvalue Problems and Generalized Sturmians. *Adv. Quantum Chem.* **2002**, *41*, 51. Preliminary research unpublished. Included as an appendix.
258. Aquilanti, V.; Cavalli, S.; Coletti, C.; Grossi, G. Alternative Sturmian Bases and Momentum Space Orbitals: An Application to the Hydrogen Molecular Ion. *Chem. Phys.* **1996**, *209*, 405.
259. Aquilanti, V.; Cavalli, S.; De Fazio, D. Hyperquantization Algorithm. I. Theory for Triatomic Systems. *J. Chem. Phys.* **1998**, *109*(10), 3792.
260. Avery, J.; Shim, R. Molecular Sturmians. Part 1. *Int. J. Quantum Chem.* **2001**, *83*, 1.
261. Avery, J.; Avery, J. The Generalized Sturmian Method for Calculating Spectra of Atoms and Ions. *J. Math. Chem.* **2003**, *33*, 145.
262. Rawitscher, G. Positive Energy Weinberg States for the Solution of Scattering Problems. *Phys. Rev. C* **1982**, *25*, 2196.
263. Rawitscher, G. Iterative Solution of Integral Equations on a Basis of Positive Energy Sturmian Functions. *Phys. Rev. E* **2012**, *85*, 026701. http://link.aps.org/doi/10.1103/PhysRevE.85.026701.

264. Ovchinnikov, S. Y.; Macek, J. H. Positive Energy Sturmian States for Two-Coulomb-Center Problems. *Phys. Rev. A* **1997**, *55*, 3605.
265. Macek, J. H.; Yu Ovchinnikov, S.; Gasaneo, G. Exact Solution for Three Particles Interacting Via Zero-Range Potentials. *Phys. Rev. A* **2006**, *73*, 032704.
266. Rotenberg, M. Application of Sturmian Functions to the Schroedinger Three-Body Problem: Elastic e+-H Scattering. *Ann. Phys. (N.Y.)* **1962**, *19*, 262.
267. Rotenberg, M. Theory and Application of Sturmian Functions. *Adv. At. Mol. Phys.* **1970**, *6*, 233.
268. Fano, U.; Cooper, J. Spectral Distribution of Atomic Oscillator Strengths. *Rev. Mod. Phys.* **1968**, *40*, 441.
269. Fernández-Menchero, L.; Otranto, S. Single ionization of $CH_4$ by Bare Ions: Fully Differential Cross Sections. *Phys. Rev. A* **2010**, *82*, 022712.
270. Granados-Castro, C. M.; Gómez, I. A.; Ancarani, L. U.; Gasaneo, G.; Mitnik, D. M. Perturbative-Generalized Sturmian Method for the Study of Photoionization in Atoms 2015. Submitted for publication.
271. Granados-Castro, C. M.; Ancarani, L. U.; Gasaneo, G.; Mitnik, D. M. Sturmian Approach to Single Photoionization of Many Electron Atoms and Molecules. *J. Phys.: Conf. Ser.* **2015**, *601*, 012009.
272. Harriman, J. Numerical Values for Hydrogen Fine Structure. *Phys. Rev.* **1956**, *101*, 594.
273. Granados-Castro, C. M.; Ancarani, L. U.; Gasaneo, G.; Mitnik, D. M. Sturmian Approach to Single Photoionization of $CH_4$. *Few-Body Syst.* **2014**, *55*, 1029.
274. Moccia, R. One-Center Basis Set SCF MO's. III. $H_2O$, $H_2S$, and HCl. *J. Chem. Phys.* **1964**, *40*, 2186.
275. Moccia, R. One-Center Basis Set SCF MO's. II. $NH_3$, $NH_4^+$, $PH_3$, $PH_4^+$. *J. Chem. Phys.* **1964**, *40*, 2176.
276. Moccia, R. One-Center Basis Set SCF MO's. I. HF, $CH_4$, and $SiH_4$. *J. Chem. Phys.* **1964**, *40*, 2164.
277. Banna, M. S.; McQuaide, B. H.; Malutzki, R.; Schmidt, V. The Photoelectron Spectrum of Water in the 30 to 140 eV Photon Energy Range. *J. Chem. Phys.* **1986**, *84*, 4739.
278. Brion, C.; Hamnett, A.; Wight, G.; Van der Wiel, M. Branching Ratios and Partial Oscillator Strengths for the Photoionization of $NH_3$ in the 15-50 eV Region. *J. Electron Spectros. Relat. Phenom.* **1977**, *12*, 323.
279. Backx, C.; der Wiel, M. J. V. Electron-ion Coincidence Measurements of $CH_4$. *J. Phys. B: At. Mol. Phys.* **1975**, *8*, 3020.
280. Randazzo, J. M.; Buezas, F.; Frapiccini, A. L.; Colavecchia, F. D.; Gasaneo, G. Solving Three-Body-Breakup Problems with Outgoing-Flux Asymptotic Conditions. *Phys. Rev. A* **2011**, *84*, 052715.
281. Cacelli, I.; Moccia, R.; Rizzo, A. Gaussian Type Orbital Basis Sets for the Calculation of Continuum Properties in Molecules: The Photoionization Cross Section of $H_2$. *J. Chem. Phys.* **1993**, *98*, 8742.